ALMA MATER STUDIORUM
UNIVERSITÀ DI BOLOGNA

DOTTORATO DI RICERCA IN

SCIENZE BIOMEDICHE E NEUROMOTORIE

Ciclo 38

Settore Concorsuale: 05/H1 - ANATOMIA UMANA

Settore Scientifico Disciplinare: BIO/16 - ANATOMIA UMANA

CDKN2A GENE FUSIONS IN GLIOBLASTOMA: VALIDATION AND FUNCTIONAL CHARACTERIZATION

Presentata da: Martina Bedeschi

Coordinatore Dottorato

Matilde Yung Follo

Supervisore

Stefano Ratti

Co-supervisore

Anna Tesei

Esame finale anno 2026

ABSTRACT

Glioblastoma, IDH-wildtype (GB), is the most aggressive primary brain tumor in adults, characterized by poor prognosis, elevated intratumoral heterogeneity, and limited therapeutic options. Despite extensive genomic profiling efforts, only a small number of GB patients currently benefit from precision oncology approaches. In this thesis, we investigated the landscape and functional relevance of gene fusions in GB, with a particular focus on *CDKN2A*-involving rearrangements as potential therapeutic target. Using RNA sequencing of patient-derived GB tissues and low-passage primary cell lines, we identified and molecularly validated two previously uncharacterized fusions, *CDKN2A–CDKN2B* and *CDKN2A–IZUMO3*. Functional assays revealed that these fusion-positive GB models exhibit enhanced sensitivity to the CDK4/6 inhibitor palbociclib, outperforming temozolomide (TMZ) in both 2D and 3D models. Further analyses showed that fusion-positive cells maintain p16/INK4A expression and undergo treatment-induced transcriptional reprogramming marked by stemness/EMT-associated markers (e.g., CD44, SNAI2). Moreover, co-culture models demonstrated that palbociclib selectively modulates the tumor–microglia axis in fusion-positive contexts, inducing TGFβ expression and increased microglial migration, suggestive of an early immunosuppressive M2-like shift. Jointly, these findings place *CDKN2A*-involving fusions as clinically actionable biomarkers with both cell-intrinsic and microenvironmental impact. Although future directions include assessing fusion prevalence in larger patient cohorts and validating therapeutic responses in orthotopic PDX systems, these findings demonstrate the feasibility of integrating fusion screening into routine GB molecular profiling, to enable more precise patient stratification and guide the rational application of targeted therapies.

Table of contents

Chapter 1: Introduction

1.1 Glioblastoma: The Challenge of a Lethal Brain Tumor

Glioblastoma, IDH wild-type (GB), classified as WHO Grade IV astrocytoma, represents the most common and most aggressive primary malignant brain tumor in adults[1]. It arises from glial cells or their precursors, specifically those of the astrocytic lineage, which normally provide support and protection to neurons within the central nervous system (CNS)[2,3] (Fig.1).

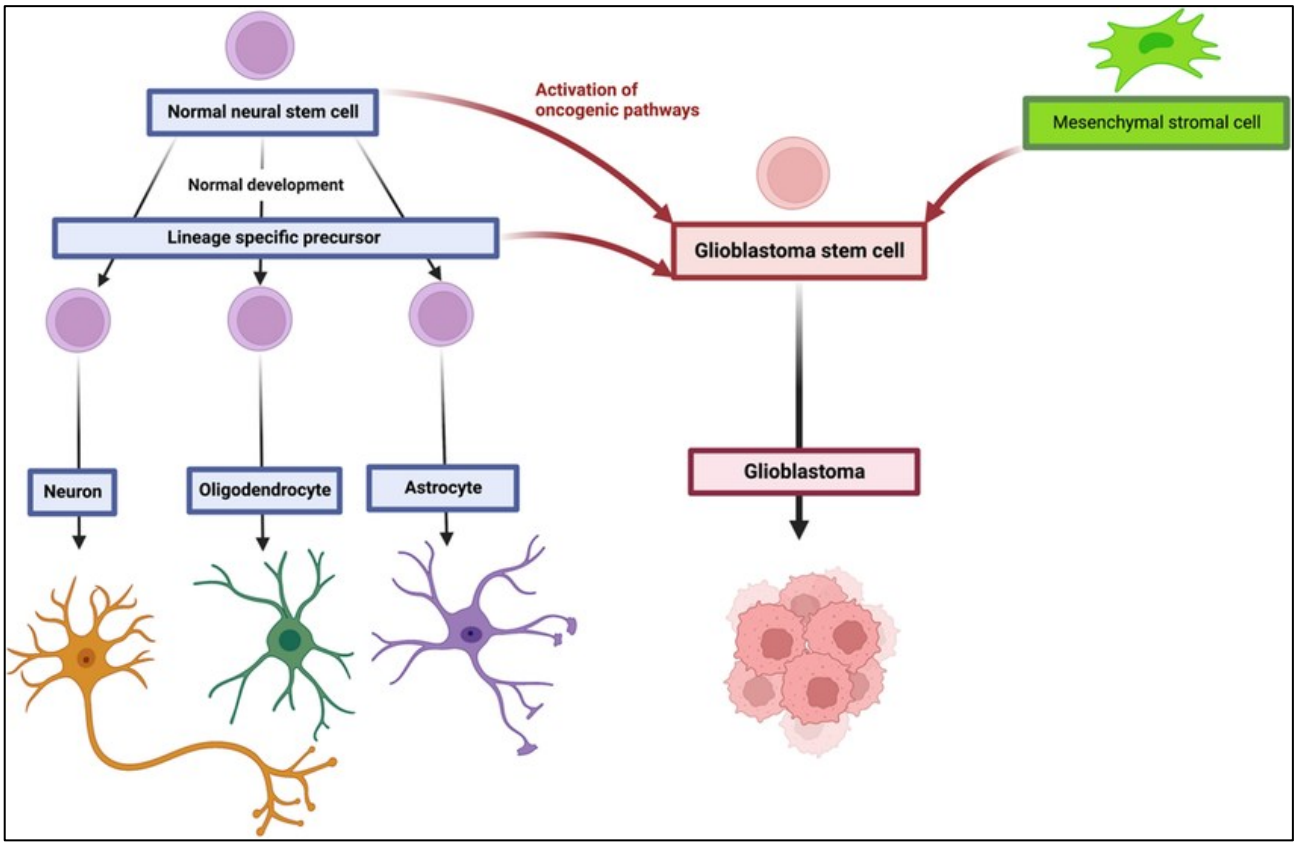

Fig.1. The origin of GB. During normal development and in the adult brain, normal neural stem cells generate glial and neuronal cells. GB stem cells may arise from neural stem cells and/or glial precursor cells through the activation of oncogenic pathways. (From Ah-Pine et al. On the origin and development of glioblastoma: multifaceted role of perivascular mesenchymal stromal cells. Acta Neuropathologica Communications. 2023[2])

GB accounts for the majority of malignant brain tumors in adults. Its incidence increases significantly with age, with a peak in individuals aged 75-84 years[1]. Despite being relatively rare compared to other systemic cancers, GB carries a disproportionately high burden of cancer mortality due to its aggressive nature and poor prognosis[1]. The prevalence is estimated at approximately 1 per 10,000 people[1].

Patients typically present with symptoms related to increased intracranial pressure (headache, nausea, vomiting), focal neurological deficits (motor weakness, sensory loss, visual changes, seizures), or cognitive/personality changes, depending on the tumor's size and location[4]. Diagnosis relies on neuroimaging, primarily contrast-enhanced Magnetic Resonance Imaging (MRI), followed by histopathological confirmation from surgical resection[5].

The current standard of care for newly diagnosed GB, established by the landmark European Organization for Research and Treatment (EORTC)/National Cancer Institute of Canada (NCIC) trial, involves maximal safe surgical resection followed by concurrent radiotherapy (fractionated focal irradiation, typically 60 Gy in 30 fractions) and chemotherapy with the alkylating agent temozolomide (TMZ), followed by adjuvant TMZ (the "Stupp protocol")[6]. Despite this aggressive multimodality treatment, the prognosis for GB patients remains extremely poor. The median overall survival is typically only 12-15 months from diagnosis[1,6]. The 5-year survival rate is less than 10%, and significantly lower (around 3%) for older adults (≥65 years)[1]. Unlike many other cancers, lifestyle modifications or early detection through screening have not demonstrated an impact on survival outcomes[1]. For all these reasons, GB remains a tremendous disease with several challenges such as high recurrence rates, treatment resistance, presence of the blood brain barrier (BBB), and an infiltrative growth. Tumor recurrence is almost inevitable, even after initial successful treatment, and recurrent GB is often more aggressive and resistant to further therapy[7]. Furthermore, GB cells exhibit significant heterogeneity and can develop resistance to both radiotherapy and chemotherapy. This resistance is driven by various factors, including genetic alterations, epigenetic modifications, and the tumor microenvironment[8]. Regarding the BBB, it restricts the entry of many therapeutic agents into the brain, limiting the effectiveness of systemic chemotherapy[9]. Lastly, the diffuse infiltration of GB cells into surrounding healthy brain tissue makes complete surgical removal impossible and contributes to recurrence[10].

GB is characterized by thorough molecular and cellular heterogeneity, both between different patients' tumors (intertumoral) and within a single tumor (intratumoral)[11]. Large-scale genomic analyses, such as The Cancer Genome Atlas (TCGA) project, have defined key genetic alterations and core signaling pathways frequently dysregulated in GB. These include:

- Receptor Tyrosine Kinase (RTK)-RAS-Phosphatidylinositol-3-OH Kinase (PI3K) pathways, such as amplification or activating mutations of epidermal growth factor (EGFR), platelet-derived growth factor receptor A (PDGFRA), MET, mutations in *PIK3CA*, *PIK3R1* and loss of *PTEN*[12,13].
- p53 pathway, such as mutations or deletions of *TP53* and amplification of *MDM2* or *MDM4*[12,13].
- Retinoblastoma (RB1) pathway, including deletion or inactivating mutations of *CDKN2A/B* (encoding p16/INK4a and p14/ARF), RB1 and amplification of CDK4, CDK6, CCND2[12,13].

Gene expression profiling initially led to the classification of GB into molecular subtypes. Firstly, in 2006, Phillips et al. defined three subtypes: Proneural, Proliferative, and Mesenchymal, using mRNA expression signatures (≈35 genes), showing different prognosis associated with neurodevelopmental gene-expression in the Proneural subtype[14].

In 2010, Verhaak et al. carried out a large-scale integrated genomic analysis via TCGA and proposed a four-subtype model (Proneural, Neural, Classical, Mesenchymal), associated with characteristic genomic aberrations (e.g. *PDGFRA*, isocitrate dehydrogenase (*IDH1*), *EGFR* amplification, *NF1* loss) and differences in survival, therapy response, and biology[15].

Subsequent works raised concerns about the Neural subtype. Indeed, analyses showed it may represent contamination from non-tumor, normal neural tissue rather than a true intrinsic tumor class[16,17]. For this reason, later studies focused on three subtypes (Proneural, Classical, Mesenchymal).

Later on, other refinements converged on methylation signatures and combining multi-omic data to delineate more stable classes[18,19]. Lastly, in 2021 the World Health Organization (WHO) has published the latest classification (fifth edition) of tumors of the central nervous system (WHO CNS5) which incorporates several molecular changes with clinicopathologic utility that are important for the most accurate classification of CNS neoplasms[3] (Fig.2).

Indeed, prior to WHO CNS5, GB was classified mainly on the basis of histology. Traditionally, GB was characterized histologically as an astrocytoma showing central pseudopalisading necrosis and abnormal microvascular proliferation under the microscope.

The WHO CNS5 classification incorporates both molecular and histological information to generate an integrated diagnosis, markedly reshaping glioma taxonomy.

Under the current criteria, GB is now defined as a diffuse astrocytic glioma that is IDH-wildtype and H3-wildtype and demonstrates at least one of the following histological or genetic features:

microvascular proliferation, necrosis, *TERT* promoter mutation, *EGFR* gene amplification, or concurrent gain of chromosome 7 and loss of chromosome 10 (+7/−10) (CNS WHO grade 4). Conversely, IDH-wildtype diffuse astrocytic tumors lacking these histological hallmarks are now categorized as molecular GB (mol-GB, WHO grade 4) if they possess any of the following alterations: *TERT* promoter mutation, *EGFR* amplification, or +7/−10 copy number changes[3,20].

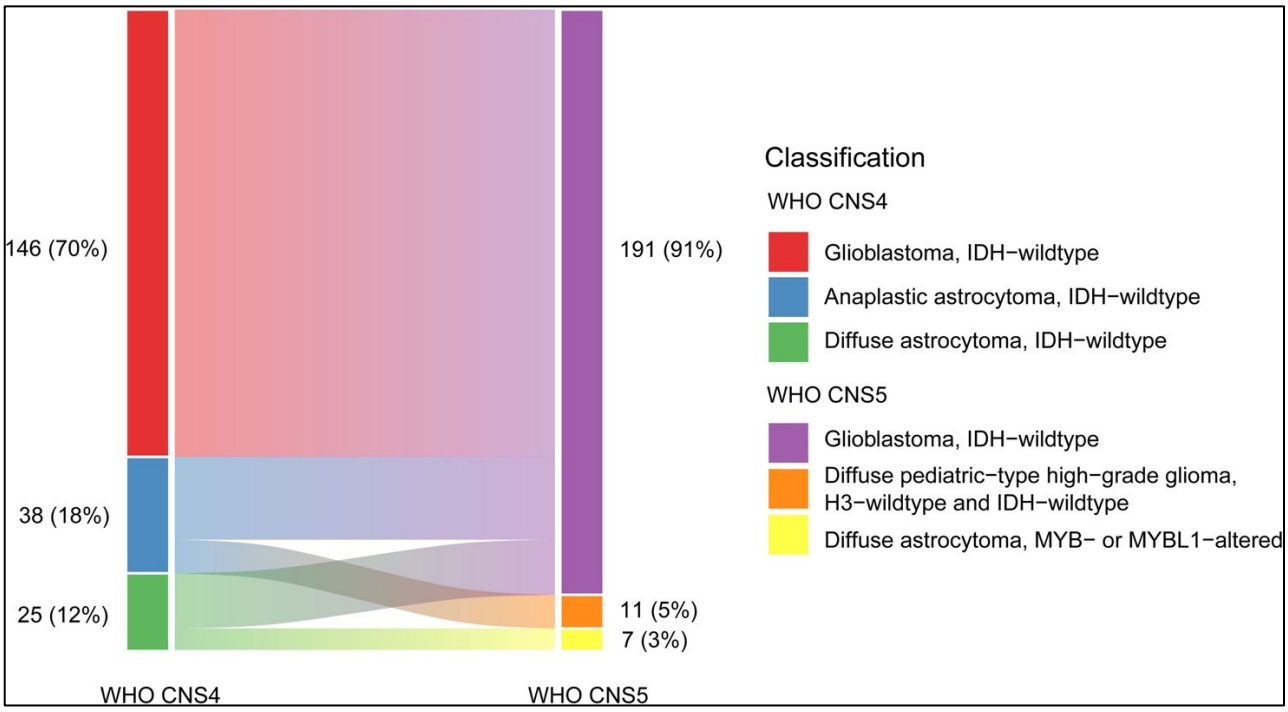

Fig.2. Changes of subtypes of IDH-wildtype diffuse gliomas from the WHO CNS4 to the WHO CNS5 classification. The blocks on the left include glioblastomas (WHO grade 4), anaplastic astrocytomas (WHO grade 3), and diffuse astrocytoma (WHO grade 2) classified using the WHO CNS4 classification system. The blocks on the right include glioblastomas, H3-wildtype and IDH-wildtype diffuse pediatric-type high-grade gliomas, and MYB- or MYBL1-altered diffuse pediatric-type astrocytomas classified using the WHO CNS5 classification system (from Guo X et al. Histological and molecular glioblastoma, IDH-wildtype: a real-world landscape using the 2021 WHO classification of central nervous system tumors. Front Oncol. 2023[20]).

However, the clinical utility of this subtyping for patient stratification and treatment remains limited, partly due to significant intratumoral heterogeneity and potential subtype switching, particularly under therapeutic pressure (e.g., mesenchymal transition associated with radiation resistance)[11,21]. Indeed, GB remains a molecularly heterogeneous malignancy that is largely refractory to current therapeutic strategies. Molecular profiling studies have demonstrated that GB exhibits substantial clonal stability throughout therapy, although distinct mutations may arise, specifically between

primary and recurrent tumors. Particularly, it was demonstrated that, although no single newly acquired or enriched genetic event predominates in recurrent glioblastomas, comparison of matched primary and recurrent tumors shows that *TERT* promoter mutations and *CDKN2A* homozygous deletions are consistently early events in gliomagenesis[22]. In contrast, alterations in other major oncogenes and tumor suppressor genes (e.g., *EGFR*, *PDGFRA*, *NF1*, *PIK3CA*, *PIK3R1*, *PTEN*) typically arise later and are often subclonal or unique to either the initial or recurrent tumor samples. These findings underscore the importance of developing therapies that target tumor cell immortalization driven by *TERT* promoter mutation and cell cycle deregulation caused by *CDKN2A* loss, as these represent the fundamental early drivers in most GBs[22].

Despite these advances in understanding GB's molecular basis, translating this knowledge into effective therapies has proven remarkably challenging, highlighting the urgent need for novel therapeutic strategies targeting distinct molecular weaknesses.

1.2 Gene Fusions: Formation, Function, and Relevance in Human Disease

The genome is a dynamic landscape shaped by diverse variations. This inherent instability is partly due to its intricate architecture, which includes large non-coding regions, repetitive elements, and specific fragile sites that are susceptible to breakage and subsequent structural alterations[23–25].
DNA replication, repair, and recombination processes, although generally high-fidelity, can occasionally undergo to errors, particularly when dealing with DNA damage or complex genomic structures. Environmental mutagens and endogenous metabolic byproducts constantly challenge DNA integrity, primarily through the induction of DNA breaks, especially double-strand breaks (DSBs), which are potent triggers for genomic rearrangements if misrepaired[26]. The cellular system responsible for maintaining genome stability, including DNA repair pathways and cell cycle checkpoints, is crucial for preventing harmful rearrangements. However, defects in these pathways, often observed in cancer, significantly increase the rate of genomic instability and the likelihood of events like gene fusions[26].

A gene fusion occurs when two distinct genes or gene fragments are joined together. This process is driven by genomic alterations such as chromosomal inversion, tandem duplication, interstitial deletion, or translocation[27]. The genes may be originally located on the same chromosome (intrachromosomal) or on different ones (interchromosomal). The fusion event can lead to the creation of a chimeric mRNA and hybrid proteins with potentially new or abnormal functions, which can play a significant role in the development of various human diseases, particularly cancers[27]. Alternatively, a gene fusion can alter gene regulation by placing one gene under the promoter or enhancer of another, causing its expression to become dysregulated. Notably, gene fusion, along with gene duplication and deletion, are common chromosomal rearrangements in cancer genomes and often precede the appearance of malignant traits[27,28].

Gene fusions represent an important class of somatic alterations in cancer. They play a significant role in the initial steps of tumorigenesis and are estimated to be responsible for 20% of global cancer morbidities. They are formed by chromosome structural variation (SV) and may result in the creation of new open reading frames (ORFs)[29].

The identification of gene fusions has become crucial in the diagnosis and prognosis of many cancers, serving as key biomarkers.

1.2.1 Mechanism of fusion formation

Multiple mechanisms can lead to the formation of fusion genes within cells. The most frequent one involves somatic chromosomal rearrangements, including four fundamental types: deletions, translocations, tandem duplications, and inversions[28] (Fig.3).

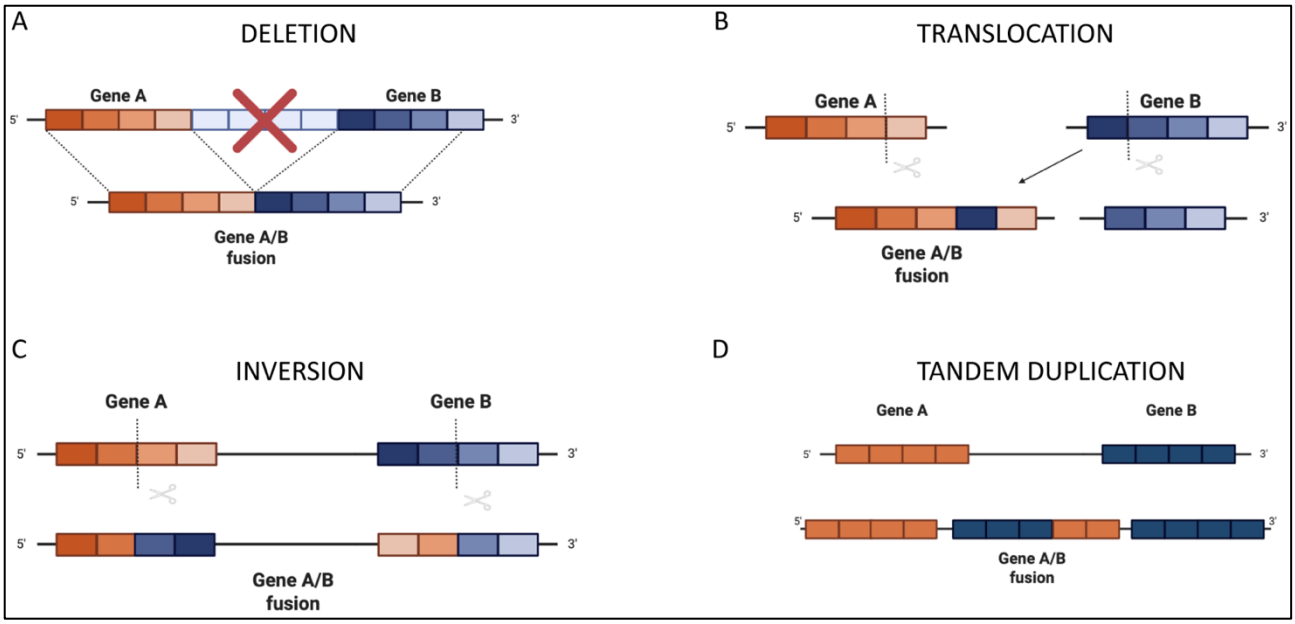

Fig.3 Most frequent chromosomal rearrangements that can led to the formation of gene fusion. A. Deletion. B. Translocation. C. Inversion. D. Tandem duplication

- Deletions: deletions of the genomic region situated between two genes on the same DNA strand can lead to the formation of a fusion gene. An example is the TMPRSS2-ERG fusion in prostate cancer. Indeed, this event results from the fusion of a promoter/enhancer region of an androgen-responsive prostate-specific serine protease 2-encoding gene, *TMPRSS2*, to the v-ets erythroblastosis virus E26 oncogene homologue, *ERG*, or the ETS variant 1 gene, *ETV1,* and over 20 other gene fusion variants. Fusion of *TMPRSS2* (21q22.2) and *ERG* (21q22.3), which are within 3 Mb of each other, results from a chromosome 21 microdeletion in approximately two-thirds of fusion cases[30].

- Translocations: a significant proportion of gene fusions result from inter-chromosomal events, involving genes located on different chromosomes. These fusion events are caused by translocations, which are reciprocal or non-reciprocal exchange of chromosomal segments between non-homologous chromosomes. They may involve the insertion of small genomic segments from one chromosome into another, or more extensive reciprocal translocations that exchange large chromosomal regions, often entire chromosome arms[28,31,32]. These rearrangements generate chimeric proteins with novel or deregulated functions, such as constitutive tyrosine kinase activity or aberrant transcriptional regulation, which drive oncogenesis through uncontrolled proliferation, inhibition of apoptosis, and altered cell differentiation[32,33].

The formation of such fusion genes is frequently associated with genomic instability and improper repair of DNA double-strand breaks, particularly via non-homologous end joining (NHEJ)[31]. Furthermore, recent advances in high-throughput sequencing technologies have revealed a far greater complexity in fusion gene architecture than previously acknowledged, uncovering numerous cryptic, complex, and multi-step translocations that eluded detection by traditional cytogenetic methods[33].

Such inter-chromosomal rearrangements are particularly common in hematologic malignancies and sarcomas, where they frequently act as primary oncogenic drivers. Indeed, the first chromosomal translocation identified in human cancer was reported in 1960, involving a reciprocal exchange between chromosomes 9 and 22 in chronic myeloid leukaemia (CML). This event led to the discovery of the Philadelphia (Ph) chromosome, a notably shortened version of chromosome 22[27,28,34]. This breakthrough paved the way for the molecular characterisation of gene fusions and translocations in the early 1980s. Specifically, the fusion of *ABL1* and *BCR* genes, resulting from the Ph chromosome, leads to constant activation of a tyrosine kinase in CML[35]. Additionally, in approximately 80% of Burkitt lymphomas, a translocation positions the *MYC* gene near highly active immunoglobulin heavy chain promoters, inducing its prolonged oncogenic expression[35].

Another well-characterised example is the *EWSR1-FLI1* fusion found in Ewing sarcoma, resulting from a t(11;22)(q24;q12) translocation[31].

- Inversions: in some cases, segments of a chromosome are reversed in orientation, causing a fusion gene through chromosomal inversion event. Usually, an inversion has occurred when a fusion involves genes located on opposite DNA strands. These genes may be oriented either toward or away from each other, and an inversion in either configuration can result in gene fusion. A defining characteristic of this fusion type is the creation of reciprocal fusion genes at both ends of the inversion[28,36]. However, due to differences in promoter activity, one or both of these reciprocal fusions may not be transcribed, making them undetectable by transcriptome sequencing. A well-known example is the *EML4-ALK* fusion gene found in non-small cell lung cancer (NSCLC), which arises from a 12 Mb inversion on chromosome 2[36]. Another example was reported by Ciampi et al.[37]. Indeed, their study identifies a novel *AKAP9-BRAF* fusion gene in papillary thyroid carcinomas, particularly in cases linked to radiation exposure. This fusion results from a paracentric inversion on the long arm of chromosome 7 [inv(7)(q21–22q34)], bringing together exons 1–8 of *AKAP9* with exons 9–18 of *BRAF*[37].

This rearrangement truncates the N-terminal regulatory region of *BRAF*, leading to a constitutively active kinase that operates independently of RAS signaling. The resulting fusion protein exhibits elevated kinase activity, induces ERK phosphorylation, and transforms cells in vitro and in vivo, confirming its oncogenic potential[37].

- Tandem Duplications: another form of chromosomal rearrangement, which can lead to fusion genes, is the tandem duplication, in which a genomic segment is duplicated and the copies are positioned adjacent to the original sequence. When the breakpoints of the duplicated region fall near existing genes, a fusion gene may form at the junction between the original and duplicated segments[28]. When two genes on the same DNA strand are involved in a fusion, tandem duplication or deletion is often the underlying mechanism. The gene order in the resulting transcript can offer an additional indication, in fact tandem duplications typically produce chimeric transcripts in which the genes appear in reverse order compared to their original genomic arrangement.

Several examples of this event are known. The study of Jones et al. identifies a recurrent oncogenic gene fusion between *KIAA1549* and *BRAF* in approximately 66% of pilocytic astrocytomas (PAs), the most common pediatric brain tumor[38]. This fusion is caused by a ~2 Mb tandem duplication on chromosome 7q34, not found in higher-grade gliomas, making it highly specific to PAs. The tandem duplication fuses parts of the *KIAA1549* gene to the kinase domain of *BRAF*, creating an in-frame fusion transcript. Several fusion variants were identified, and all of them retain the active *BRAF* kinase domain, but lack its N-terminal autoinhibitory region, leading to constitutive activation of *BRAF* signaling[38].

Other examples of tandem duplication are reported in colorectal (CRC) and lung cancer by Lipson et al. Indeed, they discovered two new gene fusions: *C2orf44-ALK* in a CRC sample and *KIF5B-RET* in a lung adenocarcinoma using next generation sequencing (NGS) on tissue samples[39]. Lastly, in 4 out of 48 glioblastoma samples was discovered and characterized the *FGFR3-TACC3* gene fusion. This fusion is caused by a 70-kb tandem duplication on chromosome 4p16.3 and, interestingly, was not found in any low-grade glioma samples[40].

A key finding is that this fusion leads to the loss of the 3'-untranslated region (3'-UTR) of *FGFR3*, which normally binds to miR-99a and regulates gene expression. The absence of the 3'-UTR in the fusion transcript allows for increased expression of the *FGFR3-TACC3* fusion gene because its activity is no longer counteracted by miR-99a, even though miR-99a is highly expressed in both normal brain and

glioblastoma. In the study it was demonstrated that the *FGFR3-TACC3* fusion protein promotes cell proliferation and tumor progression in cultured glioblastoma cells and in a mouse xenograft model[40].

In summary, the formation of fusion genes arises through various chromosomal rearrangements, each contributing distinct structural alterations to the genome. Deletions, translocations, inversions, and tandem duplications represent the principal mechanisms driving these events, often resulting in the creation of chimeric proteins with aberrant or constitutively active functions. Indeed, gene fusions are not merely genomic curiosities, they are potent drivers of various human diseases, most notably cancer, but also certain developmental disorders[41]. These fusions play a critical role in tumorigenesis across diverse cancer types, frequently serving as oncogenic drivers and diagnostic biomarkers. In fact, the resulting chimeric proteins often possess altered signaling properties, enzymatic activity, localization, or stability compared to their wild-type counterparts. For instance, many fusion proteins involving tyrosine kinases lead to constitutive activation, driving uncontrolled cell proliferation and survival independent of normal growth factor signaling[41]. Other fusions might involve transcription factors, resulting in aberrant gene expression programs that contribute to tumorigenesis[41].

This growing understanding highlights the dynamic and intricate nature of genome organization in cancer and underscores the biological and clinical importance of studying gene fusions.
Advances in high-throughput sequencing technologies have significantly enhanced our ability to detect both common and complex fusion events, deepening our understanding of their biological impact and potential as therapeutic targets.

1.2.2 Functional Consequences of Gene Fusions

The assembly of two previously independent genes through chromosomal rearrangements can result in extensive functional repercussions that drive oncogenesis. As mentioned before, among the most well-known outcomes of gene fusions is the formation of chimeric proteins that exhibit altered or novel functions. These fusion proteins can disrupt cellular homeostasis through various mechanisms. For example, gene fusions involving protein kinases frequently result in constitutive activation of

signaling pathways. This occurs when the 5' fusion partner provides a dimerization domain that forces ligand-independent activation of the kinase domain of the 3' partner[42].

Several examples are known. *BCR-ABL1* in CML is one of that. The fusion, which encodes a constitutively active tyrosine kinase that persistently activates downstream effectors such as the MAPK, PI3K/AKT, and JAK/STAT pathways, drives cell proliferation and survival[35,43].

Another case is *EML4-ALK* fusion, found in NSCLC, which leads to constitutive ALK kinase activity and is responsive to targeted ALK inhibitors[36,44]. In addition, *NPM-ALK* assembly, present in most anaplastic large cell non-Hodgkin's lymphomas, combines the nucleolar phosphoprotein (NPM) oligomerization domain with the ALK kinase, resulting in constitutive dimerization and activation[45].

Lastly, *FGFR3-TACC3* is a fusion identified in glioblastoma and bladder cancer, and results in persistent activation of FGFR3 signaling and mitotic spindle defects due to TACC3-mediated microtubule interaction[40]. It was demonstrated that the expression of these fusion proteins in astrocytes and mice brains leads to the formation of glioma-like tumors, showing an invasive and highly proliferative behavior[46].

On the other hand, fusions involving transcription factors often produce chimeric proteins with dysregulated DNA-binding or aberrant transcriptional activity. Notably, *EWSR1-FLI1*, the hallmark fusion of Ewing sarcoma, encodes an oncogenic transcription factor that reprograms gene expression by binding GGAA-microsatellite sequences and activating genes involved in invasion and proliferation[31,47]. Another example is *PML-RARA* fusion, found in acute promyelocytic leukemia (APL). This fusion creates a dominant repressor complex and disrupts retinoic acid signaling, impairing myeloid differentiation[48]. Similarly, *TMPRSS2-ERG* fusion, frequent in prostate cancer, results in *ERG* overexpression and disruption of differentiation and cell adhesion programs[30].

Fusion proteins can also be directed to new subcellular localizations. Such displacement has the capability to introduce proteins to previously not present substrates or biochemical contexts. Indeed, *FIG-ROS1* fusion, where *FIG* (Fused in Glioblastoma) is normally associated with the Golgi apparatus, alters ROS1 kinase localization to the Golgi, modifying its signaling dynamics and oncogenic potential[49].

Finally, fusion proteins can gain entirely new functions absent in the original partner genes. Furthermore, they can also interfere with the activity of wild-type proteins. Particularly, the *BCR-*

ABL1 fusion protein not only gains constitutive kinase activity but also disrupts cytoskeletal architecture and adhesion, enhancing the invasive potential of leukemic cells[43].

In addition, in some gene fusion events, the main consequence is not the generation of a chimeric protein but the dysregulation of gene expression. It is the case of proto-oncogenes which became under the control of highly active promoters or enhancers. The *IGH-MYC* translocation in Burkitt lymphoma[32,50,51] and the *TMPRSS2-ERG* fusion in prostate cancer[30,52] are some examples.

These regulatory fusions do not require the generation of corrupted proteins to exert oncogenic effects as the altered expression of the target gene is sufficient to disrupt cellular differentiation and homeostasis.

1.2.3 Relevance in Human Disease

Gene fusions are critical in the diagnosis, prognosis, and treatment of various human diseases. Indeed, they serve as biomarkers for the detection of specific cancer types and can supply targets for therapeutic interventions.

In oncology, their importance is multi-faceted as they can act as oncogenic drivers, inducing or promoting tumor development and progression. Furthermore, many fusions are highly specific to certain cancer subtypes (e.g. *BCR-ABL1* in CML, *PML-RARA* in APL, *EWSR1-FLI1* in Ewing sarcoma), making them essential for accurate diagnosis[31,43,48,53]. In addition, the presence or absence of specific gene fusions can correlate with disease aggressiveness and poor patient outcome, serving as a prognostic indicator[54]. Lastly, fusion proteins, particularly kinases, can be considered great targets for specific inhibitors. Indeed, the success of imatinib against *BCR-ABL1* changed CML treatment and paved the way for targeted therapies against other fusions[55].

The detection of gene fusions using NGS has significantly improved our understanding of disease pathogenesis and continues to reveal novel diagnostic, prognostic, and therapeutic opportunities, particularly in cancer.

1.3 The Landscape of Gene Fusions in Cancer

Cancer is essentially a disease of the genome, defined by the accumulation of genetic and epigenetic variations that drive uncontrolled cell growth, invasion, and metastasis. While point mutations and copy number alterations have long been recognized as key oncogenic events, the contribution of structural variations, particularly gene fusions, has gained increasing attention with the advent of NGS technologies[32,44].

Gene fusions, resulting from chromosomal rearrangements, play a significant role in the development and progression of various cancers[32]. These aberrant hybrid genes often encode fusion proteins with altered functions, leading to the disruption of normal cellular processes and the promotion of tumorigenesis. For that matter, as discussed earlier, gene fusions can act as potent oncogenic drivers across a wide spectrum of human malignancies, including carcinomas, hematological disorders and sarcomas[32,44,56].

The oncogenic potential lies primarily in the creation of chimeric proteins that disrupt normal cellular processes. Particularly, the impact of fusion proteins on proto-oncogenes and tumor suppressor genes is noteworthy. Proto-oncogenes are normal genes that regulate cell growth and differentiation. When involved in gene fusions, they can be placed under the control of promoters or enhancers from their fusion partner, leading to their overexpression. Alternatively, the fusion event can result in a constitutively active protein product, independent of normal regulatory mechanisms. This gain-of-function often transforms the proto-oncogene into an oncogene, driving uncontrolled cell proliferation and survival[32]. On the other hand, tumor suppressor genes normally inhibit cell growth and promote apoptosis. Gene fusions involving tumor suppressor genes can lead to their inactivation through several mechanisms. The fusion event might disrupt the coding sequence of the tumor suppressor gene, resulting in a non-functional protein. Alternatively, the fusion protein might acquire a dominant-negative activity, interfering with the function of the normal protein produced by the remaining allele. Loss of tumor suppressor function removes critical brakes on cell growth, contributing to cancer development[32]. Ultimately, fusions involving receptor tyrosine kinases often result in ligand-independent dimerization and constitutive kinase activity, leading to persistent activation of downstream signaling pathways (e.g., *BCR-ABL1* (CML), *EML4-ALK* (NSCLC))[35,36,43].

The identification of specific gene fusions has profound clinical implications in cancer. Indeed, not only certain fusions are pathognomonic or highly characteristic of specific cancer subtypes, aiding in

accurate diagnosis and classification, but can also correlate with patient prognosis and predict response to therapy.

In this light, NGS-based methods, particularly RNA sequencing (RNA-seq), have become powerful tools for the systematic discovery and detection of gene fusions, revealing a complex landscape across diverse tumor types[44]. Databases cataloging known and novel fusions are continuously expanding, providing valuable resources for research and clinical practice[57].

As mentioned earlier, gene fusions are implicated in a wide range of cancers. In hematological malignancy one of the most common gene fusion is *TEL-AML1* (*ETV6-RUNX1*) in childhood B-cell acute lymphoblastic leukemia (B-ALL) and it is the results of the translocation t(12;21)(p13;q22). The *TEL-AML1* fusion protein acts as an aberrant transcription factor, disrupting normal hematopoietic development[58]. Another example is *AML1-ETO* (*RUNX1-ETO*) fusion in AML, which arises from the translocation t(8;21)(q22;q22) and encodes a chimeric transcription factor that impairs myeloid differentiation[59]. Regarding solid tumors, the most well-known gene fusions are *EML4-ALK* in NSCLC[32] and *FGFR3-TACC3* in GB[60].

1.4 Pharmacological approaches in the treatment of fusion-induced cancers

Oncogenic gene fusions can be found in a broad range of cancers and are specific feature of some cancer types. Importantly, fusion-caused neoplasms tend to react well to targeted therapies; for this reason, gene fusions are important targets for cancer therapy[54].

Several drugs have been already developed to target these specific alterations. As an example, Imatinib (Glivec, Novartis) is used to treat BCR-ABL fusion protein in CML. Additionally, Axitinib (Inlyta, Pfizer) is able to target ALK fusion, particularly in NSCLC. Indeed, it inhibits multiple receptor tyrosin kinases including VEGFR, PDGFR and c-KIT. Other ALK inhibitors are used to treat NSCLC fusions such as Crizotinib (Xalkori, Pfizer) or Ceritinib (Zykadia, Novartis).

In addition to drugs specifically targeting gene fusions, various drugs targeting the pathways regulated by the genes involved can also be used[54]. An example is palbociclib, which is a selective inhibitor of cyclin-dependent kinases 4 and 6 (CDK4/6). It is primarily known to be used for hormone receptor-positive breast cancer (alone or in combination with aromatase inhibitors or tamoxifen),

thanks to its ability to block cell cycle in the G1 phase, wich is essential in hormone receptro-positive breast cancer[65].

However, the role of palbociclib in other neoplasm types is developing. Recently, in metastatic NSCLC with *EGFR* mutation, *PIK3CA* mutation and *CDK4* amplification, has benefited from a combination therapy of osimertinib and palbociclib after disease progression on treatment with osimertinib alone[66].

Furthermore, palbociclib has been evaluated in head and neck cancers with *CDKN2A* alterations[67]. In this light, while direct studies on palbociclib for GB are limited[68], CDK4/6 inhibitors have been explored due to their potential to target signaling pathway in this disease[69]. The treatment landscape for cancers associated with gene fusions is expanding rapidly, with targeted therapies such as TKIs and specific inhibitors offering promising outcomes for patients. For these reasons, the identification of gene fusions is crucial for tailoring appropriate therapies.

1.5 Gene Fusions in Glioblastoma: Emerging Drivers and Therapeutic Targets

While GB is classically characterized by aneuploidy, copy number alterations, and point mutations, the role of gene fusions as oncogenic drivers in this disease is increasingly recognized[44,70,71]. Indeed, the intrinsic genomic instability of GB cells promotes the chromosomal rearrangements necessary for fusion events[72]. These fusions often involve key oncogenic pathways already known to be dysregulated in GB, particularly those involving kinases. As outlined earlier, fusions involving the Fibroblast Growth Factor Receptor family (FGFR1, FGFR2, FGFR3) are among the most well-characterized in GB. The *FGFR3-TACC3* fusion, typically arising from a tandem duplication on chromosome 4p16.3, is recurrently found in a subset (approx. 3%) of GB cases[46,56,73]. This fusion generates a chimeric protein where the *TACC3* coiled-coil domain mediates dimerization and constitutive activation of the *FGFR3* kinase domain, leading to oncogenic signaling[46,56,60]. Beyond standard signaling, Frattini et al. demonstrated a role for *FGFR3-TACC3* in regulating mitotic spindle orientation and cellular metabolism, highlighting diverse functional consequences[74]. The presence of *FGFR* alterations, including fusions, identifies patients who might benefit from FGFR inhibitors currently in clinical development[74]. Additionally, while infrequent in adult GB (<<1%), fusions involving the Neurotrophic Tyrosine Receptor Kinase genes (*NTRK1, NTRK2, NTRK3*) are more

common in pediatric high-grade gliomas and represent a paradigm for targeted therapy as tumors harboring these fusions are highly sensitive to TRK inhibitors (larotrectinib, entrectinib) regardless of tumor histology[75,76].

Furthermore, fusions involving the *MET* proto-oncogene, encoding another RTK, have been identified in GB, potentially leading to ligand-independent activation and driving oncogenesis[54,57].

Despite it all, challenges remain. Detecting reliable fusions requires robust methodologies, often RNA-seq combined with sophisticated bioinformatics analysis pipelines, followed by orthogonal validation (e.g., FISH, RT-PCR, Sanger sequencing)[76].

In summary, even if gene fusions may not be as frequent in GB as in some other malignancies, the identification of recurrent fusions has opened new avenues for understanding GB biology and developing targeted therapeutic strategies for a subset of patients. Comprehensive genomic profiling is crucial for identifying these actionable alterations and advancing personalized medicine in the treatment of this challenging disease.

Chapter 2: Thesis Aims and Outline

The dismal prognosis of glioblastoma, IDH wild-type underscores the urgent need for novel therapeutic strategies grounded in a deeper understanding of its molecular drivers. Gene fusions represent a class of oncogenic alterations that, while perhaps less frequent than point mutations or copy number changes in GB, can create potent, targetable vulnerabilities. This thesis aimed to investigate the landscape and functional significance of gene fusions in GB, with the overarching goal of identifying novel therapeutic targets.

The comprehensive aim of this research was to identify and functionally characterize gene fusions that may serve as novel therapeutic targets in GB. This study proceeded through an integrated, multi-phase approach combining bioinformatics, molecular biology, and preclinical experimentation.

Phase 1: Literature Review and Data Mining

The initial objective was to conduct a comprehensive review of current scientific literature and publicly available genomic databases in order to critically assess and summarize the landscape of gene fusions previously reported in GB and other cancers. This phase aimed to consolidate existing knowledge on the structure, frequency, and functional roles of known fusion transcripts, particularly those with oncogenic potential or therapeutic relevance.

Phase 2: Sample Collection, Extraction, and Sequencing

Following the literature analysis, experimental work involved the collection of GB patient derived tissues obtained during neurosurgical procedures, with informed consent and ethical approval. Tissue samples were digested to obtain established GB patient-derived cell lines. RNA was extracted from both these cell lines and from freshly resected tumor tissues. RNA extracted from these specimens was subjected to NGS to identify potential fusion events. The sequencing pipeline was optimized to maximize the sensitivity for detecting rare or novel fusions.

Phase 3: Computational Analysis and Molecular Validation

Bioinformatic pipelines with fusion-calling algorithms was employed to process and analyze the sequencing data. This allowed for the detection, annotation, and prioritization of candidate fusion transcripts within the GB samples. Particular attention was given to fusions involving kinase domains, transcription factors, or other functionally significant regions. The most promising candidates, selected based on structural plausibility, recurrence, and potential druggability, were further validated through independent techniques, including PCR, followed by Sanger (capillary) sequencing to confirm breakpoint accuracy and transcript integrity.

Phase 4: Functional Characterization in Preclinical Models

The final phase of the project focused on assessing the biological and therapeutic relevance of the validated gene fusions. GB cells containing a confirmed, potentially druggable fusion protein were cultivated and used for in vitro tests, such as cytotoxicity assays, western blot analysis, gene expression analysis and migration assay. The objective was to assess the impact of pharmacological inhibition on cell viability, signaling pathways, and gene expression.

Overall Objective

The ultimate goal of this research was to discover novel gene fusions that gave rise to hybrid proteins with oncogenic activity and therapeutic potential in glioblastoma. By integrating genomic profiling with functional validation and pharmacological testing, this study aimed to contribute to the development of targeted treatment strategies for this highly aggressive brain tumor.

This introduction has provided an overview of gene fusions, their role in cancer, the clinical challenge posed by GB, and the emerging importance of gene fusions within this specific disease context. The subsequent chapters will detail the methodologies employed and the results obtained in the pursuit of identifying and characterizing therapeutically relevant gene fusions in glioblastoma.

Chapter 3: Materials and methods

3.1 RNA extraction and sequencing

Total RNA was extracted from both primary GB tissue samples and cell lines using AllPrep DNA/RNA mini kit (Qiagen, Hilden, Germany) according to the manufacturer's instructions. Samples were processed under RNase-free conditions to prevent RNA degradation. The quantity and purity of the isolated RNA were assessed using a NanoDrop spectrophotometer and a Qubit fluorometer (Thermo Fisher Scientific, Waltham, NA, USA), and RNA integrity was evaluated using the Agilent 2100 Bioanalyzer (Agilent Technologies, Santa Clara, CA, USA).

For RNA sequencing, library preparation was performed. Libraries were quantified using a Qubit fluorometer (Thermo Fisher Scientific, Waltham, NA, USA) and validated for quality using the Agilent 2100 Bioanalyzer (Agilent Technologies, Santa Clara, CA, USA).

Sequencing was performed on Illumina platform (Illumina, San Diego, CA, USA). Raw sequencing reads were subjected to quality control, followed by adapter trimming and low-quality base removal.

Clean reads were aligned to the human reference genome. Read counts were normalized for downstream analyses.

3.2 Gene fusion detection

Fusion calls were done on RNA-Seq data with four different tools:

- STAR-Fusion v1.6.0[73]
- FusionCatcher v1.20[78]
- RNA-Seq Alignment v1.1.1, Illumina Basespace (now only v2.0.2 is available) (https://emea.illumina.com/products/by-type/informatics-products/basespace-sequence-hub/apps/rna-seq-alignment.html)

- TopHat Alignment v1.0.0, Illumina Basespace (now removed)[79]

The results were harmonized, integrated and annotated with an in-house downstream pipeline (written in Python) to find a consensus and prioritize candidate fusion genes. The following criteria were followed for downstream filtering:

- fusions with a consensus of at leat 3 out of 4 callers
- fusions co-occurring in both a tissue sample and its derived cell line
- fusions not detected in healthy brain samples (from the online datasets, E-MTAB-4519, E-GEOD-64810, which were downloaded and analyzed with our fusion-calling pipeline)
- fusions detected with a frequency < 10% among the tumor samples

Circos plots were generated with the Circos v0.69.8[80]

3.3 Gene fusion validation

Reverse transcription (RT) reactions were performed to obtain cDNA using SuperScript VILO cDNA Synthesis kit (Thermo Fisher Scientific, Waltham, MA, USA). Polymerase chain reaction (PCR) primers were designed to amplify fragments containing the fusion boundary detected by RNA-seq using Primer3Web (Supplementary Table 1). FastStart High Fidelity PCR System (Roche, Basel, Switzerland) was used for PCR reactions. Products were purified with the QIAquick PCR purification kit (Qiagen, Hilden, Germany) and extraction of specific bands was performed with the QIAquick Gel Extraction kit (Qiagen, Hilden, Germany). PCR products were sequenced by Sanger Sequencing using the Big Dye Terminator v3.1 Cycle Sequencing kit (Applied Biosystems, Foster City, CA, USA).

3.4 Cell Culture and In Vitro Conditions

Patient-derived tumor samples were collected under a protocol approved by the Italian Local Ethics Committee (CEROM IRST IRCCS-AVR, protocol code: IRST B004). All patients provided written informed consent prior to surgery. Tumor specimens were pathologically confirmed as grade IV glioblastoma. Tumor specimens were obtained from 4 GB patients treated at Bufalini Hospital. All the samples were collected at initial diagnosis and were used to derive G63, G65, G41 and G48 cell lines.

Freshly resected tumor tissues were rinsed and processed via mechanical dissociation with sterile bisturi followed by enzymatic digestion using collagenase (Gibco™, Thermo Fisher Scientific, Waltham, MA, USA), DNase I (Roche, Basel, Switzerland) and hydrocortisone (Stemcell Technologies, Vancouver, Canada) at 37 °C for up to 2 hours. The resulting single-cell suspensions were cultured in specific neurosphere medium supplemented with 20 ng/mL epidermal growth factor (EGF; Sigma-Aldrich, Merck, Darmstadt, Germany), 10 ng/mL fibroblast growth factor (FGF; Sigma-Aldrich, Merck, Darmstadt, Germany), 1% penicillin/streptomycin (Gibco™, Thermo Fisher Scientific, Waltham, MA, USA) and 2% amphotericin B (Euroclone, Milan, Italy). Cultures were maintained under hypoxic conditions (1% O_2) in a humidified incubator at 37 °C and 5% CO_2. All primary GB cell lines were routinely screened for mycoplasma contamination using the MycoAlert™ Mycoplasma Detection Kit (Lonza, Basel, Switzerland).

Microglia cell line (CHME-5) was obtained from the American Type Culture Collection (ATCC, Manassas, UA, USA). The cell line was maintained as a monolayer at 37 ◦C in hypoxic conditions. CHME-5 cells were cultured in Dulbecco's Modified Eagle Medium (Thermo Fisher Scientific, Waltham, NA, USA) and passed every 2-3 days.

Glioblastoma Stem-like Cell Cultures (GSCs)

GSC cultures required 3–4 weeks to establish. Once established, cells were maintained by mechanical dissociation and propagated as neurospheres in a humidified hypoxic incubator at 37 °C with 5% CO_2.

3.5 *In vitro* cytotoxicity assay

For 2D culture cytotoxicity assay, cells were collected, counted and seeded at a density of 2000 cells per well in a 96 well plate (Corning, Corning, NY, USA). For 3D culture cytotoxicity assay, cells were collected, counted and seeded at a density of 1000 cells per well in a 384 ultra low attachment well plate. After 24h or 7 days from the seeding, drugs were added at different concentrations. 2D and 3D cell viability was measured using the CellTiter 96® AQueus One Solution Cell Proliferation Assay and CellTiter-Glo® 3D Cell Viability Assay (Promega, Milan, Italy) respectively. For the 2D cell cultured, viability measurements were collected after 24-48-72h from drug administration. CellTiter 96® reagent was added to each well and the absorbance signal was read after 2h using SinergyH1 reader (Biotek). Regarding the 3D cell culture, spheroids were removed from the 384-well low-attachment culture plates and placed separately in single wells of a 96-well opaque culture plate (Corning, USA). CellTiter-Glo® 3D reagent was added to each well and the luminescence signal was read after 30 min using the BioTek SinergyH1 reader. All experiments were conducted at least in triplicate.

3.6 Co-culture method

Co-culture of GB patient-derived spheroids and CHME-5 cell line was performed in a 1:1 ratio; CHME-5 cells were added immediately after the drug treatments. The co-cultures were performed with permeable support for 6-well plate 0.4 µm transparent PET membrane insert (Corning, Corning, NY, USA). After 48h RNA was extracted both from GB and CHME-5 cells as previously described.

3.7 Migration assay

GB patient-derived cells were seeded in the in a 24 multiwell plate. After 7 days, palbociclib and TMZ were added to the culture medium and CHME-5 cells were seeded onto the membrane of the 24-well transwell insert (8 µm pore size). After 48h hours, the medium was removed from the insert and, after washing with PBS, crystal violet 0.5% in methanol was added to each insert. After 30 minutes, the wells were washed with demineralized water and any non-migrated cells from the apical side of the transwell insert membrane was gently removed using a cotton-tipped applicator.
Images were taken with Olympus IX51 microscope (Olympus, Tokyo, Japan) and Nikon Digital Sight DS-U3 camera, with NIS Elements software (Nikon, Tokyo, Japan).

3.8 Western blot analysis

Briefly, cell proteins were extracted with RIPA Lysis Buffer (Thermo Fisher Scientific, Waltham, MA, USA) supplemented with Halt Protease Phosphatase Inhibitor Cocktail (Thermo Fisher Scientific Waltham, MA, USA). Mini-PROTEAN TGX™ precast gels (4–20%) (Bio-Rad Laboratories, Hercules, CA, USA) were run using Mini-PROTEAN Tetra electrophoresis cells and then electroblotted by Trans-BlotTurbo™ Mini PVDF Transfer Packs (Bio-Rad Laboratories, Hercules, CA, USA). The unoccupied membrane sites were blocked with EveryBlot Blocking Buffer (Bio-Rad Laboratories, Hercules, CA, USA) to prevent nonspecific binding of antibodies and probed with specific primary antibodies overnight at 4 °C. This was followed by incubation with the respective secondary antibodies (Table 1). The antibody-antigen complexes were detected by chemiluminescence with Clarity™ Western ECL Substrate (Bio-Rad Laboratories, Hercules, CA, USA) or in fluorescence. All experiments were conducted in triplicate.

Antibody	Supplier	Catalog Number	Application
p16 INK4A (Clone D7C1M)	Cell Signaling	80772	WB
p53 (clone DO-1)	Santa Cruz	sc-126	WB
β-Tubulin (Clone D2N5G)	Cell Signaling	15115	WB
GAPDH (Clone OTI2D9), HRP	Origene	TA802519B	WB
Anti-mouse IgG, HRP conjugated	Santa Cruz	sc-2005	WB
Anti-rabbit IgG, HRP conjugated	Santa Cruz	sc-2004	WB

Table 1. Summary table of antibody used

3.9 Digital Droplet Polymerase Chain Reaction (ddPCR)

Total RNA was extracted from cell lines using TRIzol® reagent (Invitrogen, Carlsbad, CA, USA) and Direct-zol RNA MiniPrep kit (Zymo Research, USA) following the manufacturer's instructions. RT reactions were performed in a 20-µL volume containing 400 ng of total RNA using iScript cDNA Synthesis kit (Bio-Rad Laboratories, Hercules, CA, USA). ddPCR analysis was performed using QX600 Droplet Digital PCR System Biorad (Bio-Rad Laboratories, Hercules, CA, USA). mRNA levels of the selected genes were assessed by multiplex ddPCR using both Biorad probes (Bio-Rad Laboratories, Hercules, CA, USA) and TaqMan assays (Thermo Fisher Scientific, Waltham, MA, USA). Gene expression was normalized with two endogenous reference genes, ACTB and HPRT, identified as the most stable genes by the geNorm VBA applet for Microsoft Excel. The analysis was performed using the QX Manager Standard Edition analysis software version 2.1.0.25 (Bio-Rad Laboratories, Hercules, CA, USA). All experiments were conducted in triplicate.

3.10 Statistical analysis

All experiments were performed at least three times, and quantifiable data were obtained from three independent biological replicates. Results are presented as mean ± standard deviation (SD). Statistical analyses were conducted using GraphPad Prism software (version 10.1; GraphPad, La Jolla, CA, USA). For comparisons between two groups, an unpaired two-tailed Student’s t-test was applied. For multiple group comparisons, one-way ANOVA was used when appropriate. ddPCR results were analyzed using the nonparametric Mann–Whitney U test and unpaired two-tailed Student’s t-test.

Statistical significance was defined as $p \leq 0.05$. The following p-value coding was used: $p \leq 0.05$ (*); $p \leq 0.01$ (**); $p \leq 0.001$ (***); $p \leq 0.0001$ (****).

Chapter 4: Results

4.1 Exploration of Gene Fusion Events in Glioblastoma Using Public Genomic Datasets

The initial phase of the project focused on the identification and characterization of gene fusion events in GB through the analysis of publicly available transcriptomic and genomic datasets. This basic step was designed to establish a comprehensive understanding of the landscape of gene fusions in GB, which may represent underexplored yet therapeutically actionable molecular alterations. Indeed, while gene fusions are well-characterized oncogenic drivers in hematological malignancies and in certain solid tumors, their role in GB remains rather less understood. Given the limited efficacy of current treatment modalities and the highly heterogeneous nature of GB, uncovering recurrent or functionally relevant fusion transcripts could provide new entry points for therapeutic intervention.

To this end, the first aim was to interrogate fusion transcript profiles in GB using open-source datasets, with the double goals of identifying both recurrent fusion events and fusions involving genes known to modulate oncogenic signaling pathways, cellular differentiation, immune evasion, or therapeutic resistance.

Using platforms such as cBioPortal, TCGA, and the Fusion Gene Annotation DataBase (FusionGDB), RNA-seq and whole-genome sequencing data from patients with primary and recurrent glioblastoma were analyzed.

Preliminary data revealed a diversified set of gene fusions in GB samples, though most were patient-specific and non-recurrent, consistent with the high inter-tumoral heterogeneity characteristic of GB. Nevertheless, several fusions involving genes of known biological relevance in glioma-genesis were identified, including:

- *FGFR3-TACC3*
- *PTPRZ1-MET*
- *NTRK2/3 fusions*
- *BCAN-NTRK1*

4.2 Transcriptomic Profiling of GB Patient-Derived Samples to Identify Fusion Events

GB patient-derived tissue samples were collected following appropriate ethical approval and informed consent. The samples were processed to generate patient-derived cell lines, which, along with matched freshly resected tumor tissues, were used as the source material for transcriptomic analysis.

Total RNA was extracted from both the primary tumor tissues and the corresponding cell lines. The extracted RNA underwent quality evaluation and was then sequenced using an optimized NGS pipeline.

The results from this sequencing analysis provided insight into the fusion landscape of GB and enabled the identification of candidate fusion events for further functional validation (Fig.4-5)

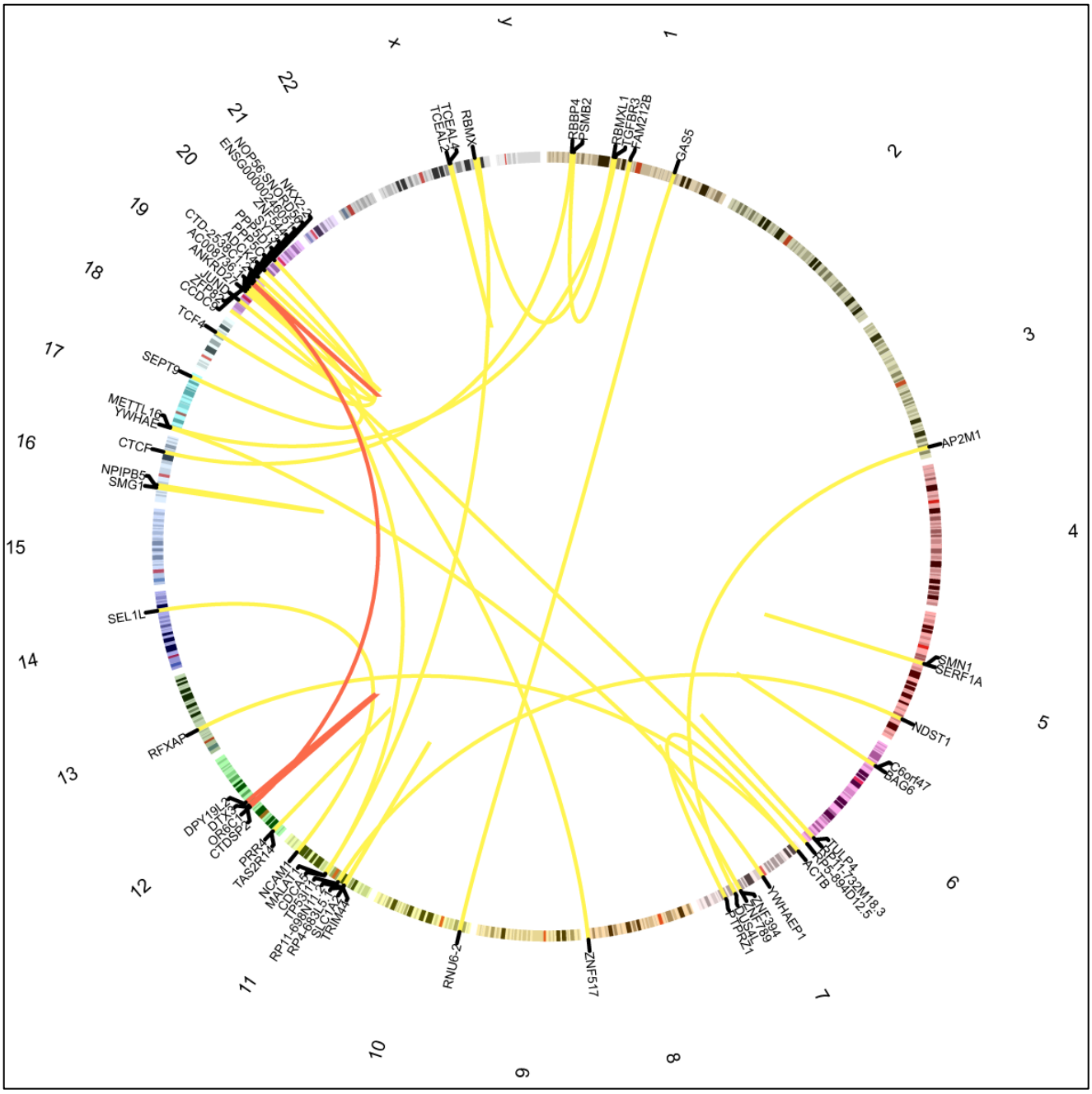

Fig.4. Representative circos plot for fusions that were found in both tissue sample and its derived cell line G63.

Fig.5 Representative circos plot for fusions that were found in both tissue sample and its derived cell line G65.

4.3 Computational Analysis

A computational analysis on fusion transcripts identified through RNA sequencing was performed. Sequencing data were processed using established bioinformatic pipelines and specialized fusion-

calling algorithms to detect, annotate, and prioritize candidate gene fusions. Particularly, four bioinformatics tools were used: FusionCatcher, RNA-Seq Alignment, STARfusion and TopHat. More than 24000 gene fusions were identified in our samples. Given the high number of elements identified, the focus was primarily directed towards fusion displayed both in tissue and cell line and the ones called by 3 or 4 of the bioinformatic tools. By this approach, around 200 fusion were screened for bibliographic study.

Each candidate fusion was evaluated based on multiple criteria, including structural plausibility, recurrence across samples, and potential druggability.

Emphasis was placed on identifying fusions involving kinase domains, transcription factors, or other regions of potential functional and therapeutic relevance. As mentioned before, particularly interesting for GB is the deletion of *CDKN2A* for gliomagenesis. Given the critical early role of *CDKN2A* loss in glioblastoma development, and supported by previous literature, gene fusions involving CDKN2A, specifically with CDKN2B (Fig.6) or IZUMO3, were selected for downstream molecular validation.

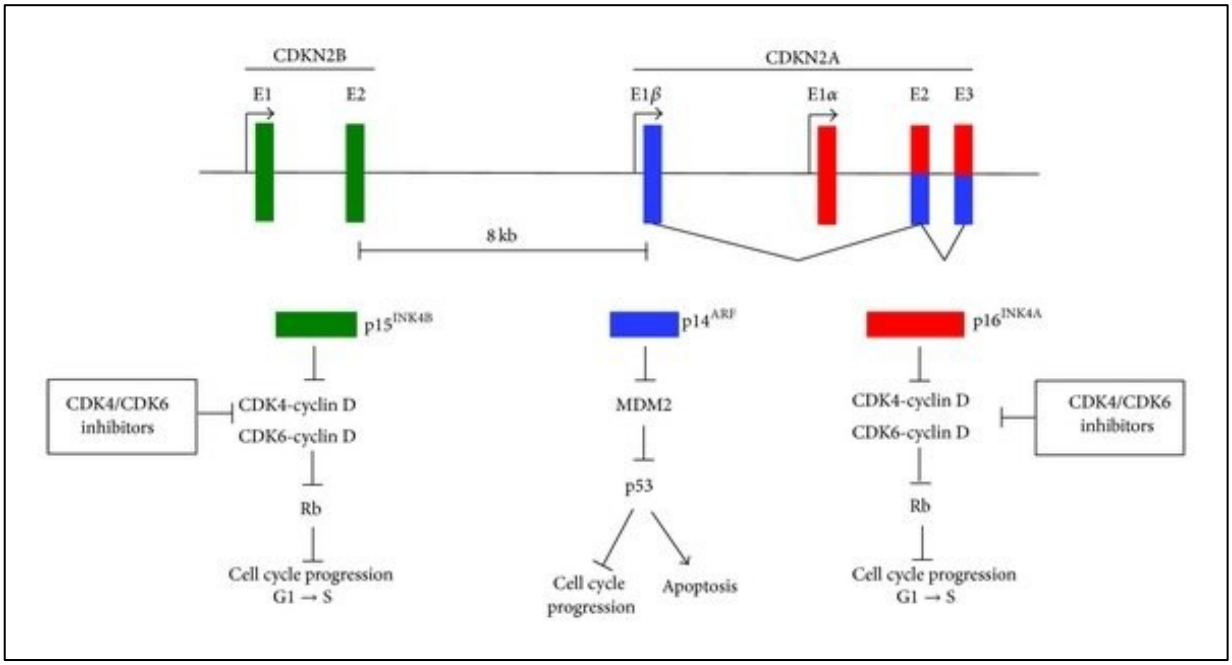

Fig.6 CDKN2A gene configuration. Genomic organization of the chromosome 9p21 which contains CDKN2B, encoding p15INK4B, and CDKN2A, encoding p14ARF and p16INK4A. p16INK4A induce cell cycle arrest by

complexing to CDK4 and CDK6 and preventing their complex formation with cyclin D. p14ARF inhibits cell cycle progression and activates apoptosis by inhibiting MDM2, which leads to activation of p53 (from Warner WA, et al. Clinicopathological and Targeted Exome Gene Features of a Patient with Metastatic Acinic Cell Carcinoma of the Parotid Gland Harboring an ARID2 Nonsense Mutation and CDKN2A/B Deletion. Case Rep Oncol Med. 2015[81])

4.4 Molecular validation of fusion transcripts

The fusions between *CDKN2A* and *CDKN2B* and between *CDKN2A* and *IZUMO3* were validated using both PCR and Sanger sequencing. A panel of GB patient-derived tissues and low-passage primary cell cultures grown under hypoxic conditions were selected for the validation. Particularly, from the tissues and primary cells were selected two fusion-positive (G63 and G65) and two -negative (G41 and G48) samples accordingly to the bioinformatic tools. The choice of two GB patient-derived tissue and cell lines without any detected fusion on the cited gene was made to compare and strengthen the model. To confirm the presence and integrity of the selected fusions, targeted PCR amplification was performed using fusion-specific primers (Fig.7), followed by Sanger sequencing to verify the breakpoint junctions and transcript structure.

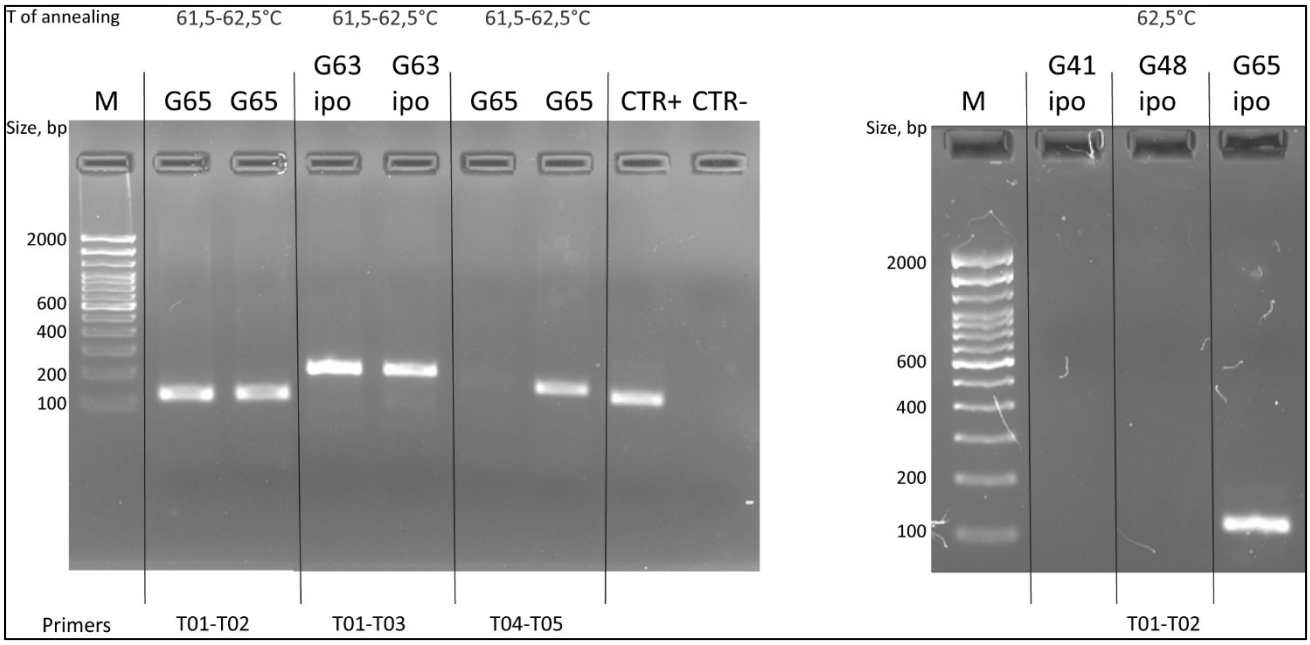

Fig.7 PCR-based validation of GB fusion transcripts in patient-derived samples. Different annealing temperature were used as long as different combination of primers. Positive and negative controls were tested as well to confirm the results. The PCR analysis was performed on G65 and G63 tissues and cell lines (IPO). The absence of the above-mentioned fusions was tested only in the cell lines sample (IPO) in G48 and G41.

Three different primer combinations were designed and tested under various annealing temperatures to optimize PCR conditions (Supplementary Table 1). The presence of the fusion transcript was successfully confirmed in the two patient-derived cell lines and their matched tissues G63 and G65, consistently with RNA-seq data. Conversely, the fusion was not detectable in G41 and G48 cell lines, in agreement with the sequencing results.

4.5 In vitro characterization of fusions in GB models and response to targeted therapy

To evaluate the biological and therapeutic relevance of the validated gene fusion, a series of in vitro experiments were conducted using GB cells expressing the confirmed fusion transcript.

The effect of TMZ, the standard of care for GB patients, was compared to palbociclib. Indeed, palbociclib is a selective inhibitor of cyclin-dependent kinases 4 and 6 (CDK4-6). The first cytotoxicity assays were performed following short-term exposure (24, 48, and 72 hours) with 3 different concentrations (0.1-1-10 µM), but neither compound showed a significant cytotoxic effect at these time points and concentrations, as measured by MTS assay, prompting a shift to prolonged exposure studies.

Extended treatment durations (6, 7, and 8 days) were subsequently tested to better capture potential delayed effects on cell viability.

Both 2D and 3D models were used for all the four patient-derived cell lines. Regarding the 2D cell culture, a differential response was observed among the cell lines tested. Indeed the IC_{50} value was reached only by G63 after 7 days of treatment with palbociclib (Fig.8), suggesting a cell line specific sensitivity. Notably, no comparable effect was detected in the earlier and later time points. This effect may suggest a balance between drug-caused cytotoxicity and adaptative cellular response. In fact, compensatory mechanism may prevent the drug activity, expecially in a 2D model which represent a simplify biological model.

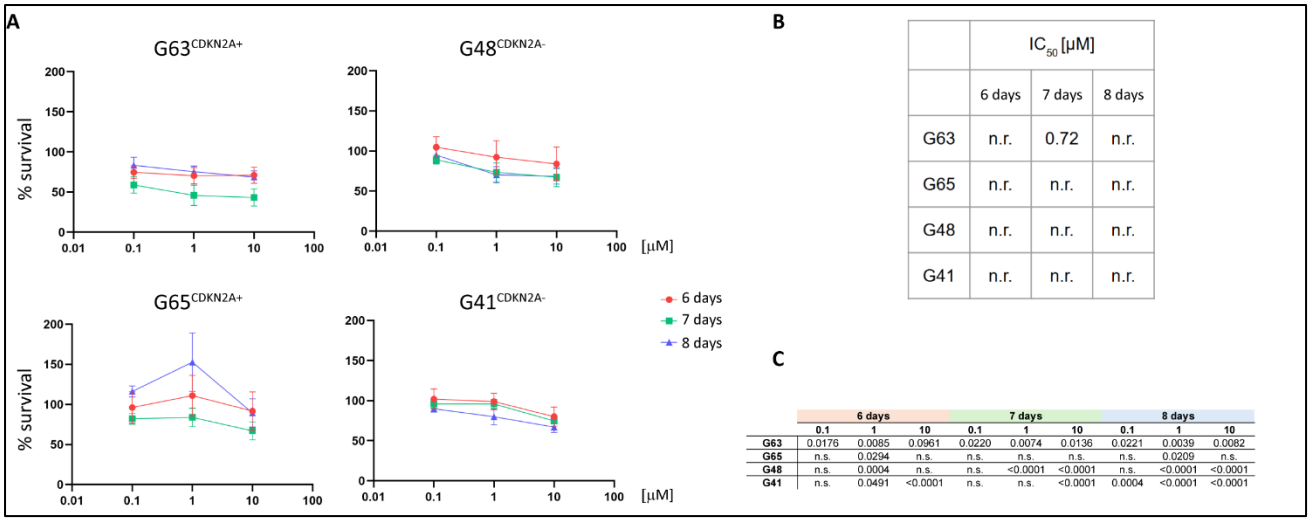

	IC50 [μM]		
	6 days	7 days	8 days
G63	n.r.	0.72	n.r.
G65	n.r.	n.r.	n.r.
G48	n.r.	n.r.	n.r.
G41	n.r.	n.r.	n.r.

	6 days			7 days			8 days		
	0.1	1	10	0.1	1	10	0.1	1	10
G63	0.0176	0.0085	0.0961	0.0220	0.0074	0.0136	0.0221	0.0039	0.0082
G65	n.s.	0.0294	n.s.	n.s.	n.s.	n.s.	n.s.	0.0209	n.s.
G48	n.s.	0.0004	n.s.	n.s.	<0.0001	<0.0001	n.s.	<0.0001	<0.0001
G41	n.s.	0.0491	<0.0001	n.s.	n.s.	<0.0001	0.0004	<0.0001	<0.0001

Fig.8 Evaluation of palbociclib effects on GB cell lines in a 2D model. A. Dose-effect curves in the four patient-derived cell lines tested. Three different concentration of palbociclib were assayed (0.1-1-10 μM) at three distinct timepoints (6-7-8 days). Data are reported as mean ± SD derived from three independent experiments. B. IC_{50} values obtained after exposure to palbociclib. C. table reporting p values for each experimental point.

TMZ did not show any efficacy in all the cell lines tested (Supplementary Fig. S1).

Following the 2D in vitro analysis, a 3D model was employed to more accurately mimic the complexity and physiological relevance of the human pathological system. After surgical removal and mechanical and enzymatic digestion, cells were cultured as neurospheres. To asses a 3D cytotoxicity assay, cells were seeded in specific ultra-low attachment plates and identical spheroids were obtained (Fig.9).

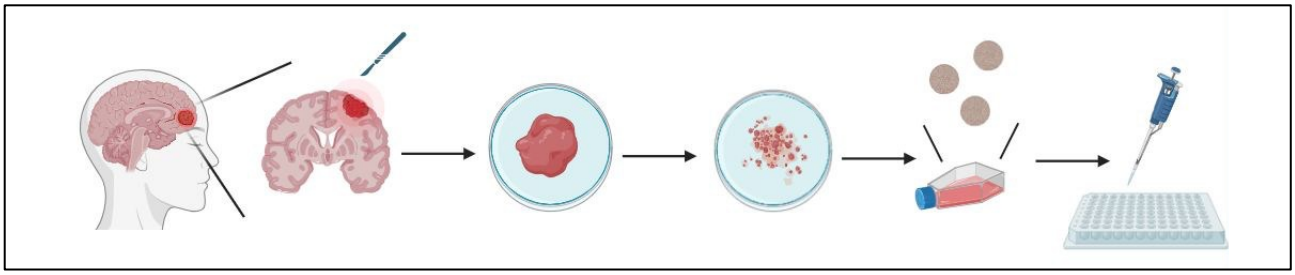

Fig.9 Graphical representation of spheroids production for 3D cytotoxicity assay.

Spheroids were exposed to increasing concentration (0.1-1-10 μM) of TMZ and palbociclib for 6-7-8 days. TMZ did not showed any efficacy in all the fusion positive cell lines. On the other hand, in the fusion negative ones, TMZ resulted more active, reaching IC_{50} values on G41 at the highest dose (Fig.10).

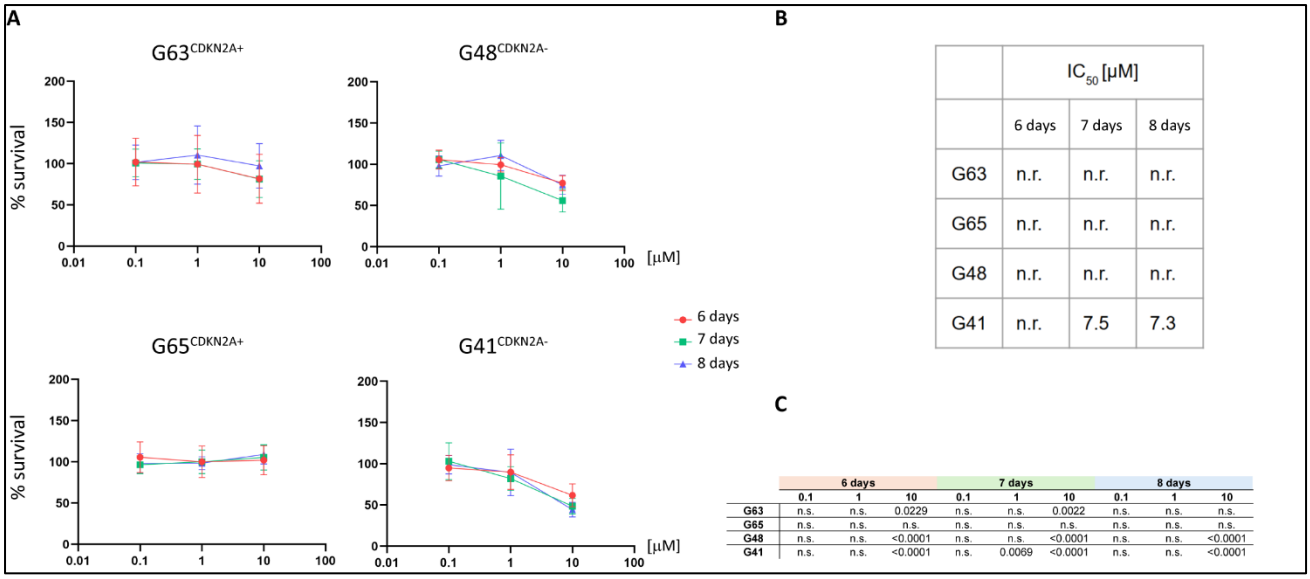

	IC50 [μM]		
	6 days	7 days	8 days
G63	n.r.	n.r.	n.r.
G65	n.r.	n.r.	n.r.
G48	n.r.	n.r.	n.r.
G41	n.r.	7.5	7.3

	6 days			7 days			8 days		
	0.1	1	10	0.1	1	10	0.1	1	10
G63	n.s.	n.s.	0.0229	n.s.	n.s.	0.0022	n.s.	n.s.	n.s.
G65	n.s.	n.s.	n.s.	n.s.	n.s.	n.s.	n.s.	n.s.	n.s.
G48	n.s.	n.s.	<0.0001	n.s.	n.s.	<0.0001	n.s.	n.s.	<0.0001
G41	n.s.	n.s.	<0.0001	n.s.	0.0069	<0.0001	n.s.	n.s.	<0.0001

Fig.10 Evaluation of TMZ effects on GB cell lines in a 3D model. A. Dose-effect curves in the four patient-derived cell lines tested. Three different concentration of palbociclib were assayed (0.1-1-10 μM) at three distinct timepoints (6-7-8 days). Data are reported as mean ± SD derived from three independent experiments. B. IC_{50} values obtained after exposure to TMZ. C. table reporting p values for each experimental point.

Regarding palbociclib, it showed a significant cytotoxic effect on all the cell lines, reaching IC_{50} values at all the timepoints tested. Particularly, the effect after 7 days was more evident in the fusion positive cell lines (with IC_{50} values ranging from 0.78 to 4.65 μM) (Fig.11). For this reason, in the subsequent experiments a 7-day treatment and a concentration of 1 μM were consistently employed.

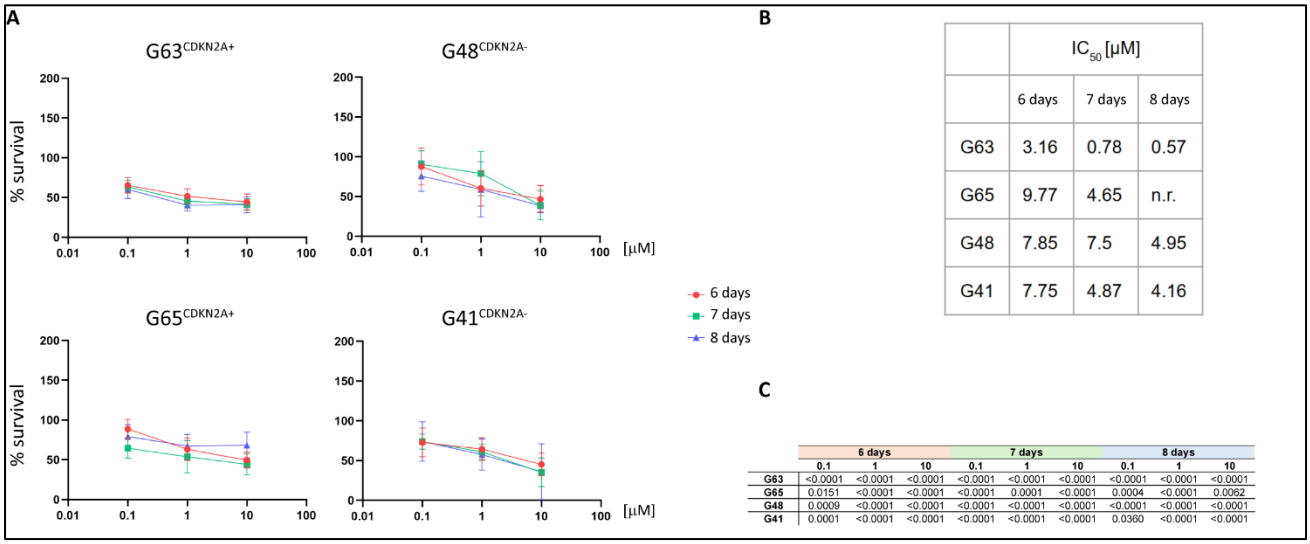

	IC50 [μM]		
	6 days	7 days	8 days
G63	3.16	0.78	0.57
G65	9.77	4.65	n.r.
G48	7.85	7.5	4.95
G41	7.75	4.87	4.16

	6 days			7 days			8 days		
	0.1	1	10	0.1	1	10	0.1	1	10
G63	<0.0001	<0.0001	<0.0001	<0.0001	<0.0001	<0.0001	<0.0001	<0.0001	<0.0001
G65	0.0151	<0.0001	<0.0001	<0.0001	0.0001	<0.0001	0.0004	<0.0001	0.0062
G48	0.0009	<0.0001	<0.0001	<0.0001	<0.0001	<0.0001	<0.0001	<0.0001	<0.0001
G41	0.0001	<0.0001	<0.0001	<0.0001	<0.0001	<0.0001	0.0360	<0.0001	<0.0001

Fig.11 Evaluation of palbociclib effects on GB cell lines in a 3D model. A. Dose-effect curves in the four patient-derived cell lines tested. Three different concentration of palbociclib were assayed (0.1-1-10 μM) at three distinct timepoints (6-7-8 days). Data are reported as mean ± SD derived from three independent experiments. B. IC_{50} values obtained after exposure to palbociclib. C. table reporting p values for each experimental point.

Interestingly, in the 3D model, the two *CDKN2A* fusion-positive cell lines demonstrated a lower sensitivity to TMZ and, for this reason, they exhibited an augmented results when treated with palbociclib, compared with the *CDKN2A* fusion-negative cell lines. In fact, the fusion-positive cell lines displayed higher difference in the response to palbociclib or TMZ in respect to the fusion-negative ones (palbociclib is 2.1 time more active in G63 and G65 compared to 1.4 in G48 and G41) (Fig.12).

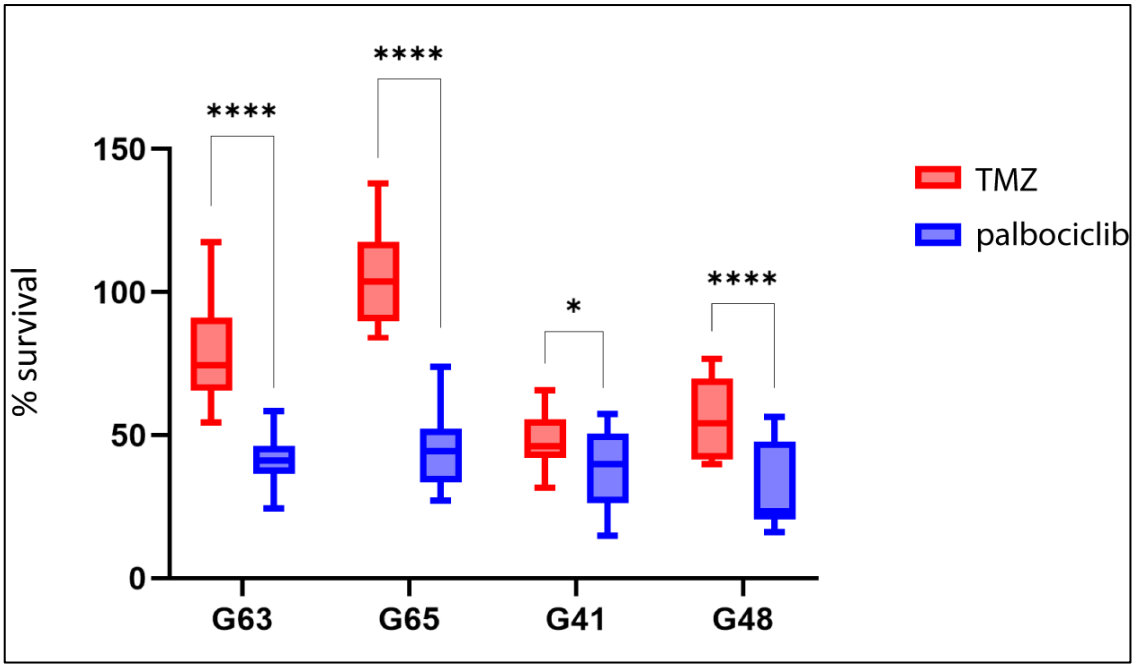

*Fig.12 Comparison between palbociclib and TMZ in inducing cell cytotoxicity in the 3D model. Patient-derived spheroids were treated with 1 μM of each drug for 7 days. Data are reported as mean ± SD derived from three independent experiments. * p<0.05, ** p<0.01, *** p<0.001, **** p<0.0001.*

In parallel, downstream analyses were conducted to determine the impact of pharmacological treatment on signaling pathways and gene expression. Western blot analysis was used to confirm changes in downstream proteins such as p16 and p53 (Fig.13), uncropped images in Supplementary

Fig. S2-3). The fusion of the gene *CDKN2A* induce an upregulation of p16, which is not present in the non-fused GB patient derived cell lines. Furthermore, p53 protein level is raised in fusion negative GB cell lines.

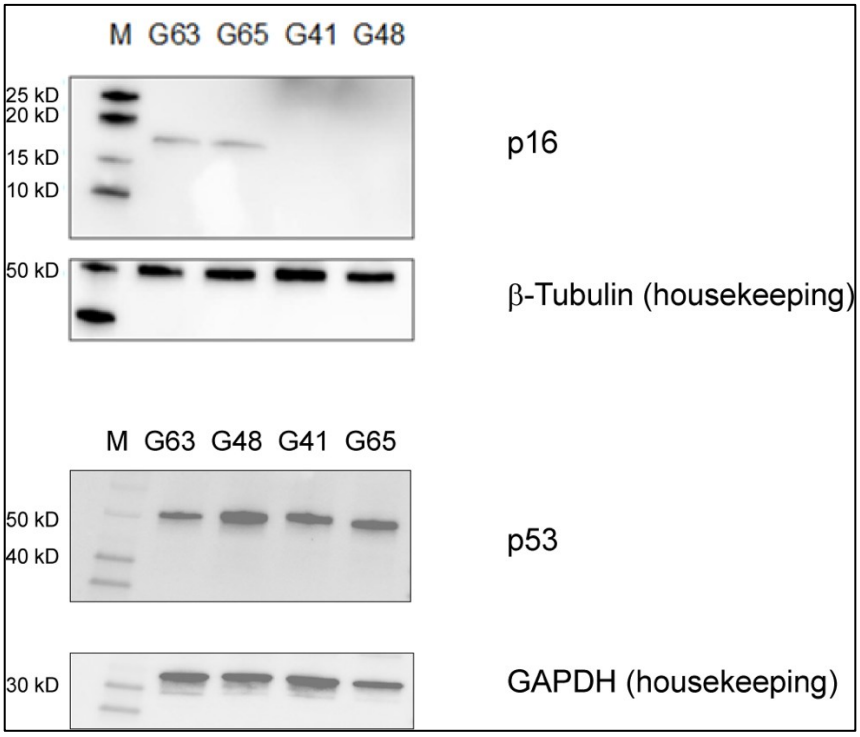

Fig.13 Western blot analysis.

Stemness profile was evaluated for all the patient-derived cell lines to investigate the role of the fusions on *CDKN2A* gene. Furthermore, quantitative PCR (qPCR) profiling was employed also to monitor transcriptional responses to treatment. Stemness profile was conducted on naïve cells and on GB cells after treatment using ddPCR technique (Fig.14-15-16). Fusion-positive cell lines showed higher stemness profile compared to the fusion-negative ones (Fig 14 A). Particularly, *SOX2* and *CD133* are significantly upregulated in G63 and G65 in respect to G48 and G41 (Fig. 14B).

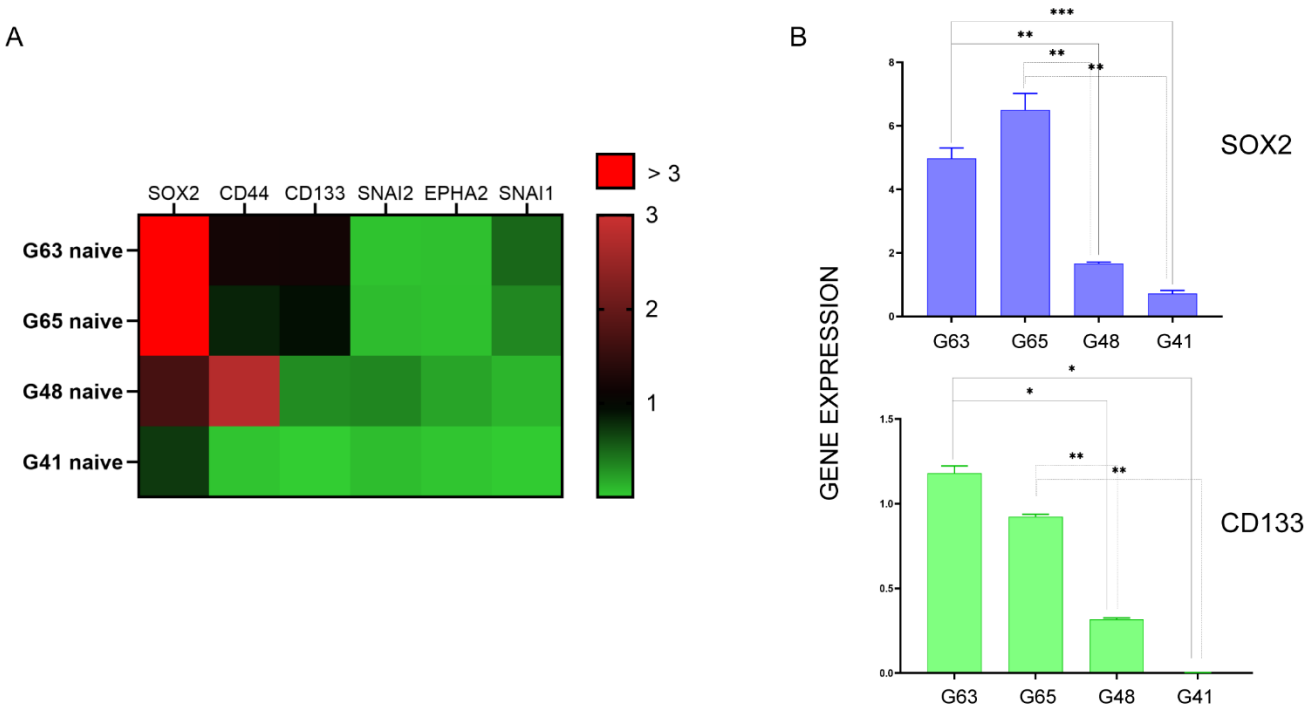

Fig.14 A. Heatmap representing gene expression analysis of stemness profile in fusion positive (G63 and G65) and fusion negative (G48 and G41) patient-derived cell lines at basal conditions using multiplex ddPCR analysis. B. Boxplots showing gene expression of SOX2 and CD133 Results are expressed as ratio after normalization on housekeeping. Data are reported as mean of three independent experiments.

Furthermore, when treated with palbociclib and TMZ, the fusion-negative cell lines display a downregulation of CD44. On the contrary, the fusion-positive cells show a significant upregulation in the expression of this marker, specifically when treated with TMZ (Fig. 15,16 and 17).

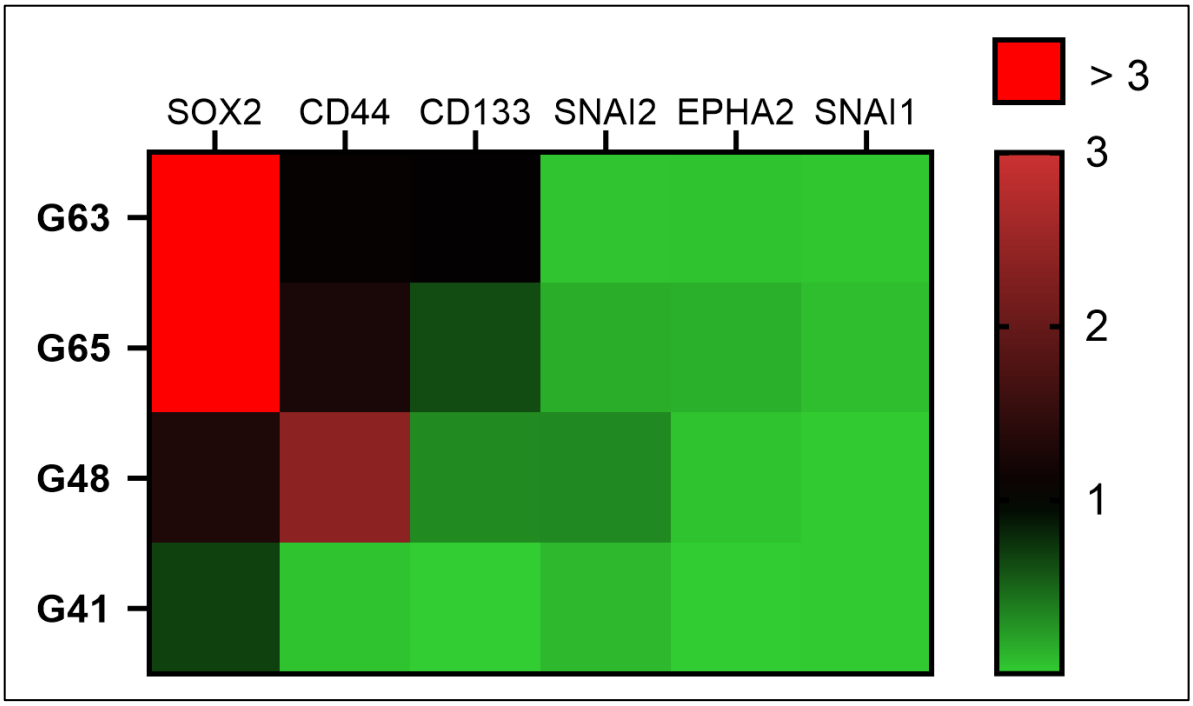

Fig.15 Gene expression analysis of stemness profile in fusion positive (G63 and G65) and fusion negative (G48 and G41) patient-derived cell lines using multiplex ddPCR analysis. Cells were exposed to palbociclib 1 μM for 7 days. Results are expressed as ratio after normalization on housekeeping. Data are reported as mean of three independent experiments.

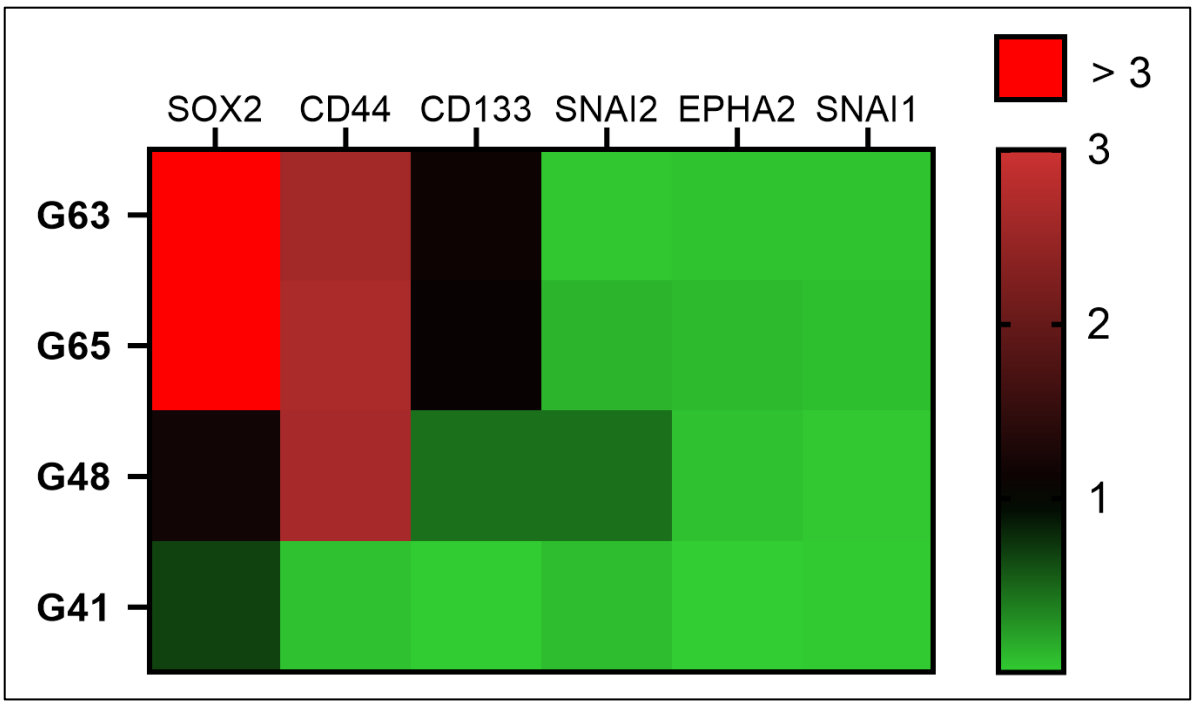

Fig.16 Gene expression analysis of stemness profile in fusion positive (G63 and G65) and fusion negative (G48 and G41) patient-derived cell lines using multiplex ddPCR analysis. Cells were exposed to TMZ 1 μM for 7 days.

Results are expressed as ratio after normalization on housekeeping. Data are reported as mean of three independent experiments.

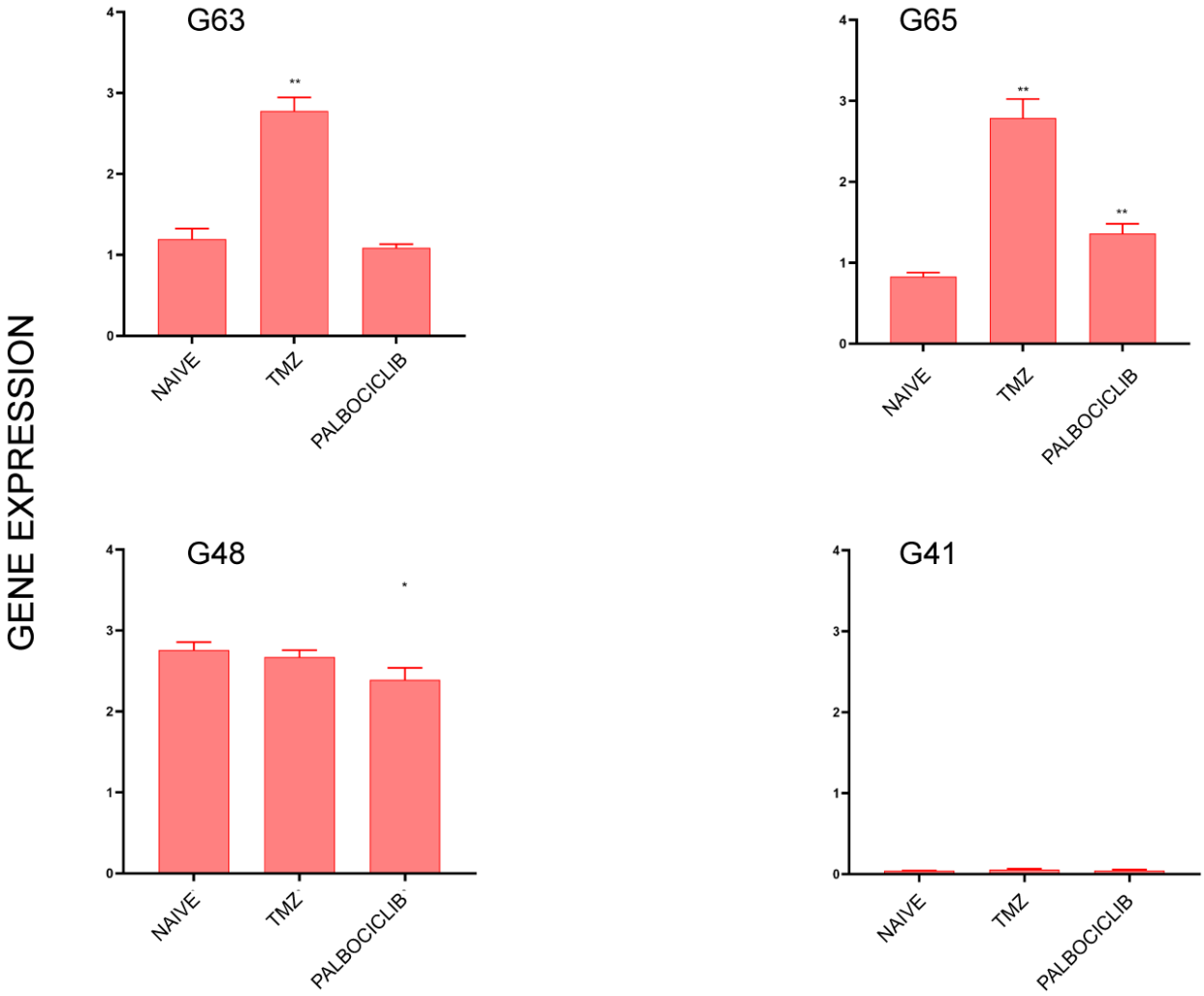

*Fig.17 Boxplot for gene expression analysis of CD44 profile in fusion positive (G63 and G65) and fusion negative (G48 and G41) patient-derived cell lines using multiplex ddPCR analysis. Cells were exposed to TMZ and palbociclib 1 μM for 7 days. Results are expressed as ratio after normalization on housekeeping. Data are reported as mean of three independent experiments. * p<0.05, ** p<0.01.*

Lastly, a co-culture model incorporating microglia was established to better replicate the cellular interactions and inflammatory environment characteristic of the human pathological system (Fig. 18 A).

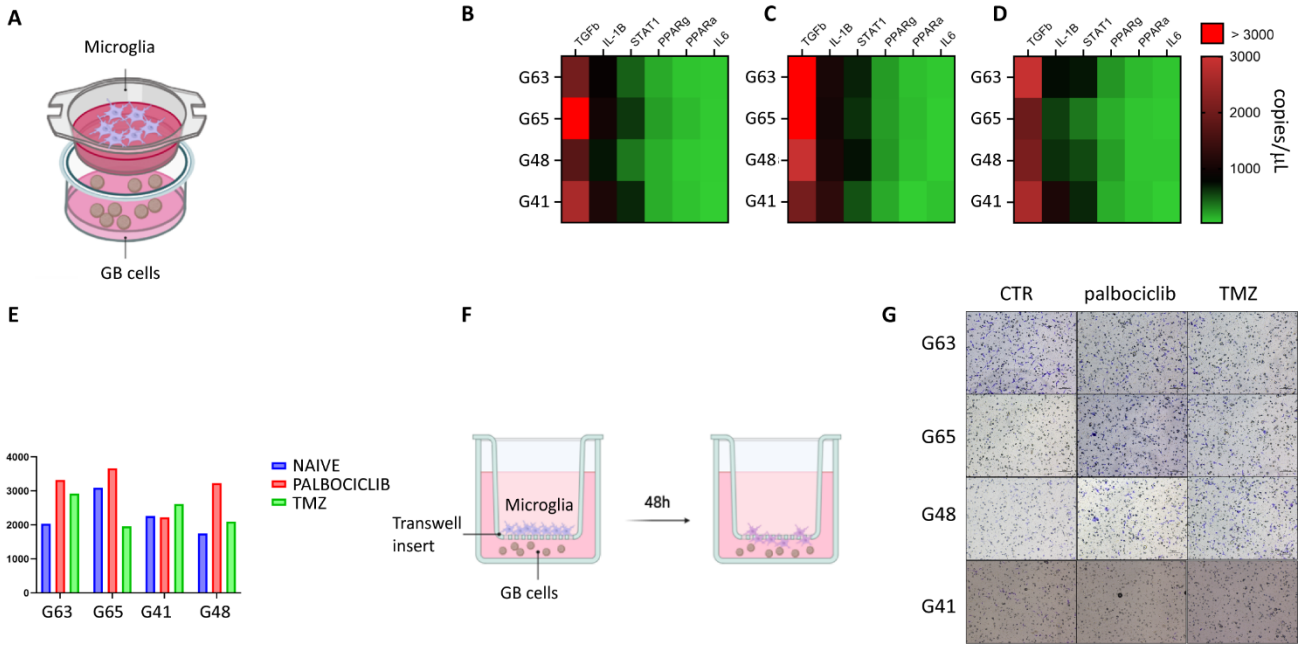

Fig.18 Microglia activation and migration in a co-culture model with patient-derived fusion-positive (G63 and G65) or negative (G48 and G41) cell lines. A. Co-culture model with GB and CHME-5 cell lines. B.C.D.E. Gene expression analysis of microglia M1 and M2 profile in fusion positive (G63 and G65) and fusion negative (G48 and G41) patient-derived cell lines using multiplex ddPCR analysis. Microglia was co-culture for 48 hours with naïve GB cells (B), GB exposed to palbociclib (C) and TMZ (D) 1 µM. E. Boxplot showing TGFβ gene expression after treatment with TMZ and palbociclib. Results are expressed as copy/µL. Data are reported as mean of three independent experiments. F. Representative migration assay using 0.8 µm inserts. G. representative images of migration assay. Microglia is colored with crystal violet when migrated towards GB cells.

GB cells were treated with 1 µM palbociclib or TMZ and co-cultured with microglia cells (CHME-5) for 48h. RNA extracted from CHME-5 cells cocultured with GB patient-derived spheroids was used to asses microglia switch from M1 to M2 with ddPCR (Fig. 18 B, C and D). No particular differences were highlighted among microglia co-cultured with non-treated GB cells, regardless of the presence of the fusion (Fig.18B). Interestingly, *TGF*β resulted upregulated mostly in fusion-positive cell lines, specifically after treatment with palbociclib (Fig.18 E). Lastly, migration assay with crystal violet was performed in the co-culture model to asses microglia activation (Fig.18 F). In G65 co-culture model, microglia is significantly migrated when treated, particularly with palbociclib (Fig. 18 G).

Chapter 5: Discussion

Glioblastoma, IDH wild-type, is the most frequent primary malignant brain tumor in adults, representing approximately 57% of all gliomas and 48% of all primary malignant CNS tumors[82]. The gold standard of care for GB is the Stupp protocol, which involves surgical resection pursued by radiotherapy and TMZ[6]. However, the substantial side effects and limited effectiveness underscore the urgent need for therapeutic advancements. Furthermore, GB presents several major challenges to effective treatment, among them its highly invasive growth into surrounding healthy brain tissue and the restrictive nature of the BBB, which limits both drug delivery and immune cell access[83,84].

Despite extensive efforts to characterize the genetic landscape of GB[13,15], these insights have yet to translate into more effective therapies. Novel treatment strategies, such as kinase inhibitors, alkylating agents, proteasome inhibitors, and transcription factor inhibitors, have failed to improve overall survival over the past two decades. Even recent advances in immunotherapy have been largely disappointing, with clinical trials evaluating PD-1 inhibitors in both newly diagnosed and recurrent GB showing no significant survival benefit[8].

Among molecular alterations, the identification and characterization of novel fusion genes hold promise for enhancing patient diagnosis and advancing precision medicine, as recently demonstrated for several newly described rearrangements[41]. Indeed, gene fusions are able to activate oncogenic pathways or disrupt tumor suppressor genes, contributing to uncontrolled cell proliferation and genomic instability.

The present thesis aieds to investigate the landscape and biological meaning of gene fusions in GB, with the comprehensive goal of identifying novel therapeutic vulnerabilities in this highly aggressive tumor type. By integrating computational analysis, molecular validation, and functional preclinical assays, we provided new insights into the role of *CDKN2A* fusions in GB biology and their potential as druggable targets.

In this study, we analyzed RNA sequencing data from patient-derived GB tissues and cell lines using bioinformatic pipelines designed to prioritize oncogenic fusion events. We identified more than 24000 gene fusions in our samples. Subsequently, we decided to focus only on fusion called by 3 or 4 of the bioinformatic tools and the one present both in tissue and cell line. We screened around 200

fusion for bibliographic study and pathway enrichment analysis. Given that *CDKN2A* is frequently mutated in gliomas, as widely reported in the literature[85–89], we directed our attention toward gene fusions in which *CDKN2A* serves as a partner gene, hypothesizing that such rearrangements may contribute to tumorigenesis or represent potential therapeutic targets. In fact, in several tumors, the defects in cell cycle are mediated by the inactivation of a region on chromosome arm 9p2, which contains the tumor suppressor gene *CDKN2A*. The fusions between *CDKN2A* and *CDKN2B* and the one between *CDKN2A* and *IZUMO3* were then validated through PCR and Sanger sequencing. We selected a panel of GB patient-derived tissues and low-passage primary cell cultures grown under hypoxic conditions. We chose two called by the bioinformatic tools for the fusions on the gene *CDKN2A* (G63 and G65). Importantly, the fusion event was confirmed in both GB patient-derived tissue and cell line. We also selected two GB patient-derived tissue and cell lines without any detected fusion on the cited gene (G41 and G48) to compare and strengthen the model. These cells were inspected for the presence of the two fusions event as well (Fig. 7).

As mentioned before, the gene *CDKN2A* encodes the cell-cycle regulator p16INK4a, which is a tumor-suppressor that restrains the progression from the phase G1 to S by inhibiting cyclin CDK4/6 complexes. Therefore, loss or disruption of *CDKN2A* releases CDK4/6 activity[90]. In this light, we decided to assess the effect of palbociclib (PD-0332991, Ibrance®) which is a selective small-molecule able to inhibit CDK4 and CDK6[91]. If the fusion leads to loss of functional p16INK4a the tumor may exhibit higher CDK4/6 activity and become more dependent on this pathway. Conversely, if the fusion either preserves p16 function, produces a dominant-negative product, or is accompanied by downstream pathway alterations, the response to palbociclib may be attenuated or absent. To validate our results, we compare the effect of palbociclib with TMZ which is the standard of care for GB. Cytotoxicity assays were performed both in 2D and 3D, in order to better resemble the structure of human tumor. In the 3D model, after 7 days of treatment, the effect of palbociclib was more visible in the fusion-positive cell lines with IC_{50} values ranging from 0.68 to 4.65 µM. Interestingly, comparing the effect of TMZ and palbociclib in both fusion positive and negative 3D models, we observed that the inhibitor of CDK4/6 was significantly more effective than TMZ in all four cell lines tested. Yet, more importantly, palbociclib demonstrated the best results over TMZ in the two fusion positive models, suggesting a new potential target for patients with fusions on *CDKN2A* gene. These results suggest that while short-term exposure to palbociclib and TMZ may not yield measurable cytotoxicity in fusion-positive GB cells, prolonged treatment, particularly with CDK4/6 inhibition, may impair

proliferation and downstream signaling, supporting the therapeutic potential of targeting this fusion in preclinical settings.

We subsequently sought to validate the findings obtained from the cytotoxicity assays by performing a western blot analysis. In particular, we investigated the expression of downstream proteins regulated by the *CDKN2A* gene to further elucidate the molecular basis of the observed responses. As expected, the cell cycle regulator protein p16/INK4A was detected exclusively in the fusion-positive cell lines, whereas it was absent in the fusion-negative models. This result is consistent with the genetic background of the analyzed cell lines and supports the hypothesis that the enhanced sensitivity to palbociclib observed in the fusion-positive models is mediated, at least in part, by the presence of functional p16/INK4A and the consequent modulation of CDK4/6 activity.

The cells were also characterized by the expression of stemness-associated features, indicative of GSC populations. These GSCs are known to reside within hypoxic and heterogeneous niches of the tumor mass, where they contribute to the remarkable aggressiveness, therapeutic resistance, and phenotypic plasticity that define clinical GB. Interestingly, non-treated fusion-positive cell lines demonstrated a more marked stemness profile compared to fusion-negative ones. In fact, *SOX2* and *CD133* are significantly upregulated in both G63 and G65 cell lines suggesting that the fusions on *CDKN2A* may reinforce stemness-associated pathways.

Cell lines were checked for stemness profile also after treatment with both palbociclib and TMZ. Unexpectedly, all the cell lines examined displayed an overall increased stemness profile following treatment with both therapeutic agents, suggesting that drug exposure, rather than simply reducing proliferative potential, may promote a compensatory shift toward a more undifferentiated and resilient cellular state. This observation aligns with the concept that anti-proliferative stress can select for, or induce, a stem-like phenotype, potentially facilitating tumor recurrence and adaptation.

Interestingly, the molecular analysis by ddPCR revealed distinct differences between fusion-positive and fusion-negative GB cell lines. While a general increase in stemness markers was observed across all samples, specific markers appeared selectively upregulated in the fusion-positive contexts, indicating that the presence of the fusion may influence the transcriptional response to therapy. In particular, *CD44*, a well-established GSC surface marker implicated in cell adhesion, migration, and therapy resistance, was significantly upregulated in fusion-positive cells, specifically after treatment

with TMZ, in contrast to fusion-negative cell lines in which CD44 is stable or has a trend of downregulation.. The upregulation of *CD44* supports the notion that fusion-positive GB cells retain, or even reinforce, their stem-like and invasive properties upon treatment, potentially contributing to the persistence of minimal residual disease. It is plausible that CDK4/6 inhibition through palbociclib triggers a selective response in these cells, promoting a cellular reprogramming process that enhances stemness and plasticity rather than purely suppressing proliferation.

To further enhance the physiological relevance of our experimental system, we established a co-culture model combining GB cells and microglial cells. This approach was designed to mimic, at least in part, the intricate crosstalk and inflammatory dynamics that occur within the GB microenvironment in vivo. The interaction between tumor and microglial cells is increasingly recognized as a key determinant of glioma progression, invasion, and therapy response. Therefore, the introduction of microglia into our model aimed to provide a more representative tool to evaluate how therapeutic interventions might influence both tumor and immune cell compartments.

In this context, while baseline M1/M2 transcriptional signatures in CHME-5 cells remained largely unaffected by the presence or absence of the fusion, the selective induction of *TGF*β expression mostly in microglia co-cultured with fusion-positive GB cells after palbociclib exposure suggests that CDK4/6 inhibition may preferentially trigger an immunomodulatory response . Interestingly, this effect was less evident under TMZ treatment, supporting the hypothesis that distinct therapeutic agents differentially shape the crosstalk between tumor and microglia (Fig.18 B, C, D and E).

The upregulation of *TGF*β and the concomitant increase in microglial migration observed particularly in the G65 co-culture following palbociclib treatment (Fig.17 G) support the hypothesis of an early M2-switch, which favors an immunosuppressive, tumor-supportive phenotype. On the other hand, the fusion-dependent nature of this response highlights an exploitable therapeutic axis, opening the path for future combinatorial strategies with microenvironment-targeted immunomodulators. Nonetheless, we also detected an activation of pro-inflammatory, M1 markers such as *STAT1* and *PPAR*γ. This activation was more pronounced upon palbociclib treatment compared to TMZ in CHME-5 cells co-cultured with fusion-positive GB cells.

While increased microglial migration might be interpreted as an indicator of heightened immune surveillance, it could also reflect the recruitment of microglia into a tumor-supportive niche, emphasizing the dual and context-dependent role of these cells in GB biology. This finding suggests that pharmacological inhibition of CDK4/6 may indirectly modulate microglial behavior, possibly through the release of chemoattractant factors such as cytokines.

Overall, these findings underscore the complexity of therapeutic responses in GB. Building on the results of this thesis, several avenues for further investigation emerge. Expanding the analysis to a larger cohort would allow for a more comprehensive assessment of fusion prevalence and recurrence in GB. Integration with additional omics layers, including DNA structural variation and proteomics, would refine our understanding of the mechanisms through which fusion events exert their effects.

Functionally, on the therapeutic side, testing additional targeted inhibitors, particularly those already approved for use in other fusion-driven cancers, could accelerate the clinical translation of our findings. Lastly, the incorporation of fusion transcript screening into routine GB molecular diagnostics could support patient stratification for future precision medicine trials.

Chapter 6: Conclusion

Glioblastoma, IDH wild-type, is the most common primary malignant brain tumor in adults, accounting for approximately 57% of all gliomas and 48% of all primary malignant tumors of the CNS[82]. The disease is characterized by a poor prognosis, with a median survival time of less than 15 months[92].

The compelling need for novel therapeutic strategies is emphasize by the dismal 5-year survival rate of just 6.6% following diagnosis[93]. Furthermore, even if extensive efforts have been made to characterize the genetic landscape of GB[13,15], these insights have yet to translate into more effective therapies.

In this light, gene fusions are gaining increasing attention in the scientific world. Indeed, gene fusions play a pivotal role in the diagnosis, prognosis, and treatment of numerous human diseases[31,43,48,53]. They function as important biomarkers for identifying specific cancer types and also represent promising targets for therapeutic intervention. One of the most recognized outcomes of such gene fusions is the production of chimeric proteins with altered or entirely novel functions. These fusion proteins can disrupt normal cellular homeostasis through multiple mechanisms. For instance, fusions involving protein kinases often lead to the constitutive activation of signaling pathways, thereby driving uncontrolled cellular proliferation[42].

In GB gene fusions are increasingly recognized as significant oncogenic contributors in this disease[44,71,72]. These fusions frequently involve key oncogenic pathways already known to be dysregulated in GB, particularly those related to kinase signaling[77].

Overall, this thesis expands the growing body of evidence highlighting the oncogenic and therapeutic significance of gene fusions in GB. While fusions involving receptor tyrosine kinases such as *FGFR, NTRK*, and *PDGFRA* have been described in subsets of gliomas, and are now targetable with FDA-approved inhibitors, the broader landscape of fusion events in GB remains poorly characterized due to technical challenges and the pronounced heterogeneity of this tumor type[94].

In this work, we identified and characterized novel *CDKN2A* fusion events, specifically *CDKN2A-CDKN2B* and *CDKN2A-IZUMO3*, using a comprehensive approach that integrated bioinformatics,

molecular validation, and functional assays. These findings lead to the evidence that GB harbors unique, often patient-specific rearrangements with potential biological and therapeutic relevance. The observation that p16/INK4A protein was detected exclusively in fusion-positive cell lines supports the hypothesis that such events disrupt cell-cycle regulation and contribute to aberrant CDK4/6 signaling.

Functionally, our data demonstrate that pharmacological inhibition of CDK4/6 with palbociclib induces a selective growth-inhibitory effect in *CDKN2A* fusion-positive GB models. Compared to TMZ, palbociclib showed greater efficacy in both 2D and 3D culture systems, underscoring its potential as a targeted therapeutic strategy in this molecularly defined subset. These findings suggest that *CDKN2A* fusions may serve as biomarkers of sensitivity to CDK4/6 inhibition, paving the way for the inclusion of such agents in precision medicine trials for GB.

Beyond cell-intrinsic effects, our co-culture experiments with microglia revealed that, even if baseline M1/M2 transcriptional programs were largely unchanged by the presence or absence of the fusion, the selective induction of *TGF*β specifically in microglia co-cultured with fusion-positive GB cells upon palbociclib treatment indicates that CDK4/6 inhibition may preferentially elicit an immunomodulatory response. Together with the increase in microglial migration, observed particularly in the G65 co-culture following palbociclib treatment, this effect is consistent with an early M2-like shift toward an immunosuppressive, tumor-supportive phenotype. Importantly, although enhanced microglial motility could reflect strengthened immune surveillance, it may equally signify recruitment into a tumor-supportive niche, underscoring the dual and context-dependent nature of microglial responses in GB. Altogether, these findings suggest that pharmacological CDK4/6 blockade can reshape microglial behavior indirectly, potentially through the release of cytokine-mediated chemoattractant signals.

Collectively, this thesis provides novel mechanistic insights into the role of *CDKN2A* fusions in GB and establishes their potential as actionable therapeutic targets. Although further validation in larger patient cohorts and in vivo models will be required, these findings demonstrate the feasibility of integrating fusion transcript screening into routine GB molecular profiling. Such an approach could ultimately enable more precise patient stratification and guide the rational application of targeted therapies, contributing to the long-term goal of improving outcomes for patients with this devastating malignancy.

Chapter 7: Future perspectives

This thesis identifies and functionally entails *CDKN2A*-involving fusions, particularly *CDKN2A-CDKN2B* and *CDKN2A-IZUMO3*, in GB. Furthermore, the present work correlates the presence of the above-mentioned fusions to preferential sensitivity to CDK4/6 inhibition (palbociclib) alongside with fusion-conditioned immuno-microenvironmental effects (e.g., *TGF*β induction in microglia and enhanced microglial migration).

In this light, two parallel hypotheses follow. On the one hand, CDKN2A fusions remodel G1/S control and dependency on CDK4/6 activity; in fusion-positive GB, CDK4/6 inhibitors are more likely to be effective, but may reprogram cells toward stemness/EMT-like states (as shown by the increased expression of *SNAI2* and *CD44*). On the other hand, CDK4/6 blockade in fusion-positive contexts may reshapes microglial behavior (early M2-like cues via *TGF*β), creating an opportunity for combinatorial strategies that oppose microenvironmental immunosuppression.

The next steps should therefore to define mechanisms of drug resistance and response and translate this knowledge into biomarker-based clinical strategies. Furthermore, it would be of great interest to verify the prevalence of the *CDKN2A* fusions in patients to understand their impact on the clinic. Since we have a local cohort of recurrent GBs (around 100 samples) and few low-grade gliomas, we could first understand the frequency of these fusions event and if differences are present between primary GBs, recurrent GBs and low-grade gliomas. Afterwards, the cohort should be expanded to better include longitudinal pairs between primary and recurrence to track also clonal stability.

Regarding the mechanism of response and resistance to inhibition of CDK4/6 with palbociclib, the future steps are to evaluate BBB penetration and test different dosing schedules (e.g., multiple administrations). In addition, fusion-negative GB cell lines should be engineered using CRISPR/Cas9 to expressed or modulate the fusions of interest and validate the results obtained. Lastly, the results would be confirmed in an orthotopic PDX mouse model.

Ultimately, we plan to better quantify stemness/EMT programs and M1/M2 profile at a single cell level in treated and untreated spheroids to identify sensitive subpopulations. In addition, stemness reversibility may be tested as well to better understand the role of a combinational therapy targeting the immune microenvironment (for example using *TGF*β pathways blockade).

In this context, we will evaluate the use of patient-derived microglia or induced-pluripotent stem cell (iPSC)-derived microglia instead of a commercial cell line and to move towards ex vivo tumor slice and PDOX mouse model to validate *TGF*β induction and migration phenotypes under CDK4/6 inhibition.

In conclusion, this thesis positions *CDKN2A*-involving fusions as actionable biomarkers in a disease where concrete signals are scarce. The priorities are clear: to validate these fusion across larger and longitudinal GB cohort and to establish their clinical prevalence across primary, recurrent, and low-grade gliomas; to functionally validate their causal role by engineering isogenic CRISPR models and confirming drug response in orthotopic PDX systems; and to mechanistically dissect both resistance and adaptive reprogramming to CDK4/6 blockade, with particular focus on stemness/EMT plasticity and microglia-mediated immunomodulation. These efforts will lay the basis for biomarker-based clinical strategies and rational combinatorial therapies, ultimately furthering the possibility of precision medicine in GB.

ABBREVIATIONS

3’-UTR: 3'-untranslated region

APL: acute promyelocytic leukemia

ATCC: American Type Culture Collection

B-ALL: B-cell acute lymphoblastic leukemia

BBB: blood brain barrier

CML: chronic myeloid leukemia

CNS: central nervous system

CRC: colorectal cancer

ddPCR: digital droplet PCR

DSBs: double-strand breaks

EGF: epidermal growth factor

EGFR: epidermal growth factor receptor

EMT: epithelial-mesenchymal transition

EORTC: European Organization for Research and Treatment

FGF: fibroblast growth factor

FIG: fused in glioblastoma

FUSIONGDB: Fusion Gene Annotation DataBase

GB: glioblastoma, IDH-wild type

GSCs: glioblastoma stem-like cells

IDH1: isocitrate dehydrogenase 1

iPSC: induced-pluripotent stem cell

MRI: Magnetic Resonance Imaging

NCIC: National Cancer Institute of Canada

NGS: next generation sequencing

NPM: nucleolar phosphoprotein

NSCLC: non-small cell lung cancer

ORFs: open reading frames

PAs: pilocytic astrocytomas

PCR: polymerase chain reaction

PDGFRA: platelet-derived growth factor receptor A

Ph chromosome: Philadelphia chromosome

PI3K: Phosphatidylinositol-3-OH Kinase

qPCR: quantitative PCR

RB1: Retinoblastoma 1

RNAseq: RNA sequencing

RTK: Receptor Tyrosine Kinase

SV: structural variation

TCGA: The Cancer Genome Atlas

TMZ: temozolomide

WHO CNS5: World Health Organization Central Nervous System fifth edition

WHO: World Health Organization

REFERENCES

1. Miller, K. D. *et al.* Brain and other central nervous system tumor statistics, 2021. *CA. Cancer J. Clin.* **71**, 381–406 (2021).

2. Ah-Pine, F. *et al.* On the origin and development of glioblastoma: multifaceted role of perivascular mesenchymal stromal cells. *Acta Neuropathol. Commun.* **11**, 104 (2023).

3. Louis, D. N. *et al.* The 2021 WHO Classification of Tumors of the Central Nervous System: a summary. *Neuro-Oncol.* **23**, 1231–1251 (2021).

4. Armstrong, T. S. *et al.* Determining priority signs and symptoms for use as clinical outcomes assessments in trials including patients with malignant gliomas: Panel 1 Report. *Neuro-Oncol.* **18**, ii1–ii12 (2016).

5. Seyhan, A. A. Circulating Liquid Biopsy Biomarkers in Glioblastoma: Advances and Challenges. *Int. J. Mol. Sci.* **25**, 7974 (2024).

6. Stupp, R. *et al.* Radiotherapy plus Concomitant and Adjuvant Temozolomide for Glioblastoma. *N. Engl. J. Med.* 10 (2005).

7. Wick, W. *et al.* NOA-04 Randomized Phase III Trial of Sequential Radiochemotherapy of Anaplastic Glioma With Procarbazine, Lomustine, and Vincristine or Temozolomide. *J. Clin. Oncol.* **27**, 5874–5880 (2009).

8. Bedeschi, M., Cavassi, E., Romeo, A. & Tesei, A. Glioblastoma Tumor Microenvironment and Purinergic Signaling: Implications for Novel Therapies. *Pharmaceuticals* **18**, 385 (2025).

9. Pardridge, W. M. The Blood-Brain Barrier: Bottleneck in Brain Drug Development. **2**, (2005).

10. Sanai, N. & Berger, M. S. Surgical oncology for gliomas: the state of the art. *Nat. Rev. Clin. Oncol.* **15**, 112–125 (2018).

11. Patel, A. P. *et al.* Single-cell RNA-seq highlights intratumoral heterogeneity in primary glioblastoma. 13 (2014).

12. The Cancer Genome Atlas Research Network. Comprehensive genomic characterization defines human glioblastoma genes and core pathways. *Nature* **455**, 1061–1068 (2008).

13. Brennan, C. W. *et al.* The Somatic Genomic Landscape of Glioblastoma. *Cell* **155**, 462–477 (2013).

14. Phillips, H. S. *et al.* Molecular subclasses of high-grade glioma predict prognosis, delineate a pattern of disease progression, and resemble stages in neurogenesis. *Cancer Cell* **9**, 157–173 (2006).

15. Verhaak, R. G. W. *et al.* Integrated Genomic Analysis Identifies Clinically Relevant Subtypes of

Glioblastoma Characterized by Abnormalities in PDGFRA, IDH1, EGFR, and NF1. *Cancer Cell* **17**, 98–110 (2010).

16. Madurga, R. *et al.* Normal tissue content impact on the GBM molecular classification. *Brief. Bioinform.* **22**, bbaa129 (2021).

17. Zhang, P., Xia, Q., Liu, L., Li, S. & Dong, L. Current Opinion on Molecular Characterization for GBM Classification in Guiding Clinical Diagnosis, Prognosis, and Therapy. *Front. Mol. Biosci.* **7**, 562798 (2020).

18. Snuderl, M. Molecular classification and deconvolution of the immune microenvironment in glioblastoma. *Neuro-Oncol.* **23**, 175–176 (2021).

19. Zhang, Y.-H. *et al.* Distinguishing Glioblastoma Subtypes by Methylation Signatures. *Front. Genet.* **11**, 604336 (2020).

20. Guo, X. *et al.* Histological and molecular glioblastoma, IDH-wildtype: a real-world landscape using the 2021 WHO classification of central nervous system tumors. *Front. Oncol.* **13**, 1200815 (2023).

21. Bhat, K. P. L. *et al.* Mesenchymal Differentiation Mediated by NF-κB Promotes Radiation Resistance in Glioblastoma. *Cancer Cell* **24**, 331–346 (2013).

22. Lucas, C.-H. G. *et al.* Longitudinal multimodal profiling of IDH-wildtype glioblastoma reveals the molecular evolution and cellular phenotypes underlying prognostically different treatment responses. *Neuro-Oncol.* **27**, 89–105 (2025).

23. Pös, O. *et al.* DNA copy number variation: Main characteristics, evolutionary significance, and pathological aspects. *Biomed. J.* **44**, 548–559 (2021).

24. Thorpe, J., Osei-Owusu, I. A., Avigdor, B. E., Tupler, R. & Pevsner, J. Mosaicism in Human Health and Disease. *Annu. Rev. Genet.* **54**, 487–510 (2020).

25. Yi, K. & Ju, Y. S. Patterns and mechanisms of structural variations in human cancer. *Exp. Mol. Med.* **50**, 1–11 (2018).

26. Chatterjee, N. & Walker, G. C. Mechanisms of DNA damage, repair, and mutagenesis. *Environ. Mol. Mutagen.* **58**, 235–263 (2017).

27. Glenfield, C. & Innan, H. Gene Duplication and Gene Fusion Are Important Drivers of Tumourigenesis during Cancer Evolution. *Genes* **12**, 1376 (2021).

28. Annala, M. J., Parker, B. C., Zhang, W. & Nykter, M. Fusion genes and their discovery using high throughput sequencing. *Cancer Lett.* **340**, 192–200 (2013).

29. Wang, Y., Shi, T., Song, X., Liu, B. & Wei, J. Gene fusion neoantigens: Emerging targets for

cancer immunotherapy. *Cancer Lett.* **506**, 45–54 (2021).

30. Barwick, B. G. *et al.* Prostate cancer genes associated with TMPRSS2–ERG gene fusion and prognostic of biochemical recurrence in multiple cohorts. *Br. J. Cancer* **102**, 570–576 (2010).

31. Mertens, F., Johansson, B., Fioretos, T. & Mitelman, F. The emerging complexity of gene fusions in cancer. *Nat. Rev. Cancer* **15**, 371–381 (2015).

32. Mitelman, F., Johansson, B. & Mertens, F. The impact of translocations and gene fusions on cancer causation. *Nat. Rev. Cancer* **7**, 233–245 (2007).

33. Meyerson, M., Gabriel, S. & Getz, G. Advances in understanding cancer genomes through second-generation sequencing. *Nat. Rev. Genet.* **11**, 685–696 (2010).

34. Rowley, J. D. A New Consistent Chromosomal Abnormality in Chronic Myelogenous Leukaemia identified by Quinacrine Fluorescence and Giemsa Staining. *Nature* **243**, 290–293 (1973).

35. Evidence of a New Chimeric bcrc-abl mRNA in Patients with Chronic Myelocytic Leukemia and the Philadelphia Chromosome.pdf.

36. Soda, M. *et al.* Identification of the transforming EML4–ALK fusion gene in non-small-cell lung cancer. *Nature* **448**, 561–566 (2007).

37. Ciampi, R. *et al.* Oncogenic AKAP9-BRAF fusion is a novel mechanism of MAPK pathway activation in thyroid cancer. *J. Clin. Invest.* **115**, 94–101 (2005).

38. Jones, D. T. W. *et al.* Tandem Duplication Producing a Novel Oncogenic *BRAF* Fusion Gene Defines the Majority of Pilocytic Astrocytomas. *Cancer Res.* **68**, 8673–8677 (2008).

39. Lipson, D. *et al.* Identification of new ALK and RET gene fusions from colorectal and lung cancer biopsies. *Nat. Med.* **18**, 382–384 (2012).

40. Parker, B. C. *et al.* The tumorigenic FGFR3-TACC3 gene fusion escapes miR-99a regulation in glioblastoma. *J. Clin. Invest.* JCI67144 (2013) doi:10.1172/JCI67144.

41. Gao, Q. *et al.* Driver Fusions and Their Implications in the Development and Treatment of Human Cancers. *Cell Rep.* **23**, 227-238.e3 (2018).

42. Saigí, M. *et al.* Biological and clinical perspectives of the actionable gene fusions and amplifications involving tyrosine kinase receptors in lung cancer. *Cancer Treat. Rev.* **109**, 102430 (2022).

43. Melo, J. V. & Barnes, D. J. Chronic myeloid leukaemia as a model of disease evolution in human cancer. *Nat. Rev. Cancer* **7**, 441–453 (2007).

44. Stransky, N., Cerami, E., Schalm, S., Kim, J. L. & Lengauer, C. The landscape of kinase fusions in cancer. *Nat. Commun.* **5**, 4846 (2014).

45. Morris, S. W. *et al.* Fusion of a Kinase Gene, *ALK* , to a Nucleolar Protein Gene, *NPM* , in Non-Hodgkin's Lymphoma. *Science* **263**, 1281–1284 (1994).

46. Singh, D. *et al.* Transforming Fusions of *FGFR* and *TACC* Genes in Human Glioblastoma. *Science* **337**, 1231–1235 (2012).

47. Riggi, N. *et al.* EWS-FLI1 Utilizes Divergent Chromatin Remodeling Mechanisms to Directly Activate or Repress Enhancer Elements in Ewing Sarcoma. *Cancer Cell* **26**, 668–681 (2014).

48. Melnick, A. & Licht, J. D. Deconstructing a Disease: RAR, Its Fusion Partners, and Their Roles in the Pathogenesis of Acute Promyelocytic Leukemia. *Blood* **93**, 3167–3215 (1999).

49. Birchmeier, C., Sharma, S. & Wigler, M. Expression and rearrangement of the ROSI gene in human glioblastoma cells. *Med. Sci.*

50. ar-Rushdi, A. *et al.* Differential Expression of the Translocated and the Untranslocated c- *myc* Oncogene in Burkitt Lymphoma. *Science* **222**, 390–393 (1983).

51. Taub, R. *et al.* Translocation of the c-mnc gene into the immunoglobulin heavy chain locus in human Burkitt lymphoma and murine plasmacytoma cells. *Proc Natl Acad Sci USA* (1982).

52. Tomlins, S. A. *et al.* Recurrent Fusion of *TMPRSS2* and ETS Transcription Factor Genes in Prostate Cancer. *Science* **310**, 644–648 (2005).

53. Testa, U. & Pelosi, E. Function of PML-RARA in Acute Promyelocytic Leukemia. in *Transcription factors in blood cell development* (eds. Borggrefe, T. & Giaimo, B. D.) vol. 1459 321–339 (Springer Nature Switzerland, Cham, 2024).

54. Liu, S. V., Nagasaka, M., Atz, J., Solca, F. & Müllauer, L. Oncogenic gene fusions in cancer: from biology to therapy. *Signal Transduct. Target. Ther.* **10**, 111 (2025).

55. Braun, T. P., Eide, C. A. & Druker, B. J. Response and Resistance to BCR-ABL1-Targeted Therapies. *Cancer Cell* **37**, 530–542 (2020).

56. Parker, B. C., Engels, M., Annala, M. & Zhang, W. Emergence of FGFR family gene fusions as therapeutic targets in a wide spectrum of solid tumours: Emergence of FGFR family gene fusions as therapeutic targets. *J. Pathol.* **232**, 4–15 (2014).

57. Sorokin, M. *et al.* Clinically relevant fusion oncogenes: detection and practical implications. *Ther. Adv. Med. Oncol.* **14**, 17588359221144108 (2022).

58. De Laurentiis, A., Hiscott, J. & Alcalay, M. The TEL-AML1 fusion protein of acute lymphoblastic leukemia modulates IRF3 activity during early B-cell differentiation. *Oncogene* **34**, 6018–6028 (2015).

59. Rejeski, K., Duque-Afonso, J. & Lübbert, M. AML1/ETO and its function as a regulator of gene transcription via epigenetic mechanisms. *Oncogene* **40**, 5665–5676 (2021).

60. Li, Y. *et al.* FGFR3-TACC3 fusion gene promotes glioblastoma malignant progression through the activation of STAT3 signaling pathway. *Front. Oncol.* **15**, 1560008 (2025).

61. Druker BJ, *et al.* Activity of a specific inhibitor of the BCR-ABL tyrosine kinase in the blast crisis of chronic myeloid leukemia and acute lymphoblastic leukemia with the Philadelphia chromosome. N Engl J Med. (2001).

62. Atkins MB, *et al.* Axitinib in combination with pembrolizumab in patients with advanced renal cell cancer: a non-randomised, open-label, dose-finding, and dose-expansion phase 1b trial. Lancet Oncol. (2018).

63. Papageorgiou S, *et al.* Alternative Treatment Options to ALK Inhibitor Monotherapy for EML4-ALK-Driven Lung Cancer. Cancers (Basel) (2022).

64. Shaw A.T. et al. Ceritinib in *ALK*-Rearranged Non–Small-Cell Lung Cancer. N Engl J Med (2014)

65. Finn RS, *et al.* The cyclin-dependent kinase 4/6 inhibitor palbociclib in combination with letrozole versus letrozole alone as first-line treatment of oestrogen receptor-positive, HER2-negative, advanced breast cancer (PALOMA-1/TRIO-18): a randomised phase 2 study. Lancet Oncol. (2015).

66. de Jager, V.D., *et al.* Osimertinib and palbociclib in an *EGFR*-mutated NSCLC with primary *CDK4* amplification after progression under osimertinib. *npj Precis. Onc.* **8**, 113 (2024).

67. Worden FP, *et al.* Palbociclib in Patients With Head and Neck Cancer and Other Tumors With *CDKN2A* Alterations: Results From the Targeted Agent and Profiling Utilization Registry Study. JCO Precis Oncol. (2024).

68. Whittaker, S., *et al.* Combination of palbociclib and radiotherapy for glioblastoma. *Cell Death Discov.* **3**, 17033 (2017).

69. Zhang J, *et al.* Multiple patient-derived glioblastoma models reveal synthetic lethality through concurrent PI3K and CDK4/6 inhibition by blocking trans-active cooperation. Neuro Oncol. (2025).

70. Duncan, C. G. *et al.* Integrated genomic analyses identify ERRFI1 and TACC3 as glioblastoma-targeted genes. *Oncotarget* **1**, 265–277 (2010).

71. Woo, H. Y. *et al.* Glioblastomas harboring gene fusions detected by next-generation sequencing. *Brain Tumor Pathol.* **37**, 136–144 (2020).

72. Mazzoleni, A. *et al.* Chromosomal instability: a key driver in glioma pathogenesis and progression. *Eur. J. Med. Res.* **29**, 451 (2024).

73. Di Stefano, A. L. *et al.* Detection, Characterization, and Inhibition of FGFR–TACC Fusions in IDH Wild-type Glioma. *Clin. Cancer Res.* **21**, 3307–3317 (2015).

74. Frattini, V. *et al.* A metabolic function of FGFR3-TACC3 gene fusions in cancer. *Nature* **553**, 222–227 (2018).

75. Manea, C. A. *et al.* A review of NTRK fusions in cancer. *Ann. Med. Surg.* **79**, (2022).

76. Torre, M. *et al.* Molecular and clinicopathologic features of gliomas harboring NTRK fusions. *Acta Neuropathol. Commun.* **8**, 107 (2020).

77. Haas, B. J. *et al.* STAR-Fusion: Fast and Accurate Fusion Transcript Detection from RNA-Seq. Preprint at https://doi.org/10.1101/120295 (2017).

78. Nicorici, D. *et al.* **FusionCatcher** – a tool for finding somatic fusion genes in paired-end RNA-sequencing data. Preprint at https://doi.org/10.1101/011650 (2014).

79. TopHat Alignment v1.0 and Cufflinks Assembly & DE v1.0 App Guide.

80. Krzywinski, M. *et al.* Circos: An information aesthetic for comparative genomics. *Genome Res.* **19**, 1639–1645 (2009).

81. Warner, W. A., Wong, D. J., Palma-Diaz, F., Shibuya, T. Y. & Momand, J. Clinicopathological and Targeted Exome Gene Features of a Patient with Metastatic Acinic Cell Carcinoma of the Parotid Gland Harboring an ARID2 Nonsense Mutation and CDKN2A/B Deletion. *Case Rep. Oncol. Med.* **2015**, 1–8 (2015).

82. Tan, A. C. *et al.* Management of glioblastoma: State of the art and future directions. *CA. Cancer J. Clin.* **70**, 299–312 (2020).

83. Drappatz, J., Norden, A. D. & Wen, P. Y. Therapeutic strategies for inhibiting invasion in glioblastoma. *Expert Rev. Neurother.* **9**, 519–534 (2009).

84. Sampson, J. H., Gunn, M. D., Fecci, P. E. & Ashley, D. M. Brain immunology and immunotherapy in brain tumours. *Nat. Rev. Cancer* **20**, 12–25 (2020).

85. Lu, V. M. *et al.* The prognostic significance of CDKN2A homozygous deletion in IDH-mutant lower-grade glioma and glioblastoma: a systematic review of the contemporary literature. *J. Neurooncol.* **148**, 221–229 (2020).

86. Lee, S. H., Kim, T. G., Ryu, K. H., Kim, S. H. & Kim, Y. Z. CDKN2A Homozygous Deletion Is a Stronger Predictor of Outcome than IDH1/2-Mutation in CNS WHO Grade 4 Gliomas. *Biomedicines* **12**, 2256 (2024).

87. Minami, J. K. *et al.* CDKN2A deletion remodels lipid metabolism to prime glioblastoma for ferroptosis. *Cancer Cell* **41**, 1048-1060.e9 (2023).

88. Noack, D. *et al.* Homozygous CDKN2A/B deletions in low- and high-grade glioma: a meta-analysis of individual patient data and predictive values of p16 immunohistochemistry testing. *Acta*

Neuropathol. Commun. **12**, 180 (2024).

89. Zhuang, D. *et al.* Prevalence and characteristics analysis of CDKN2A/B deletion in glioma. *J. Clin. Oncol.* **41**, e14026–e14026 (2023).

90. analysis of the p16 gene.pdf.

91. Liu, M., Liu, H. & Chen, J. Mechanisms of the CDK4/6 inhibitor palbociclib (PD 0332991) and its future application in cancer treatment (Review). *Oncol. Rep.* https://doi.org/10.3892/or.2018.6221 (2018) doi:10.3892/or.2018.6221.

92. Ostrom, Q. T. *et al.* CBTRUS Statistical Report: Primary Brain and Other Central Nervous System Tumors Diagnosed in the United States in 2012–2016. *Neuro-Oncol.* **21**, v1–v100 (2019).

93. Low, J. T. *et al.* Primary brain and other central nervous system tumors in the United States (2014-2018): A summary of the CBTRUS statistical report for clinicians. *Neuro-Oncol. Pract.* **9**, 165–182 (2022).

94. Reardon, D. A. *et al.* Effect of Nivolumab vs Bevacizumab in Patients With Recurrent Glioblastoma: The CheckMate 143 Phase 3 Randomized Clinical Trial. *JAMA Oncol.* **6**, 1003 (2020).

SUPPLEMENTARY

TARGET GENES	PRIMER NAME	FORWARD PRIMER	REVERSE PRIMER	LENGHT (nt)	Tm (°C)
CDKN2A-CDKN2B	T01/T03	CCCAACGCACCGAATAGTTA	TCATCATGACCTGGATCGGC	20	58-60
CDKN2A-IZUMO3	T01/T02	CCCAACGCACCGAATAGTTA	CAGACATCGAGAAGCTTGCC	20	58-59
CDKN2A-IZUMO3	T04/T05	CCGCTTCCTAGAAGACCAGT	CAGACATCGAGAAGCTTGCC	20	58

Table S1. Summary table of primers used for PCR validation of GB patient-derived tissues and cell lines

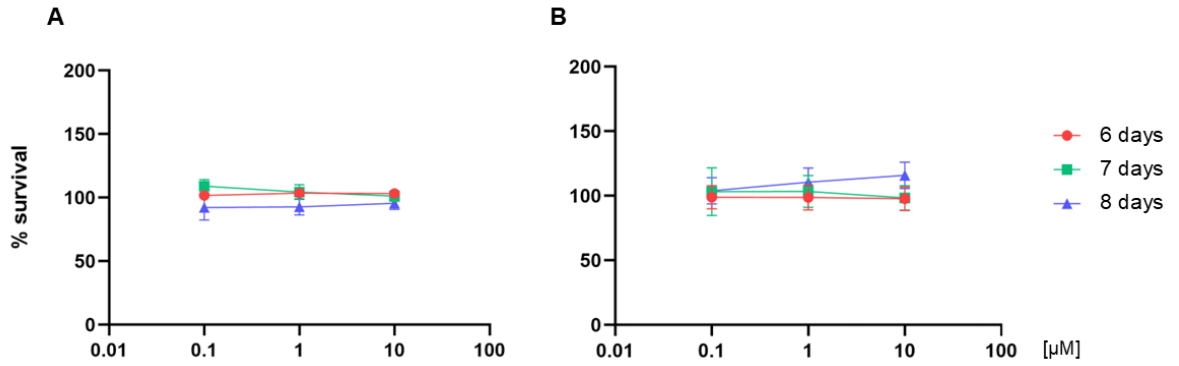

Fig. S1 Representative curves for the evaluation of temozolomide effects on GB cell lines in a 2D model (A. G63 and B. G65). Three different concentration of TMZ were assayed (0.1-1-10 µM) at three distinct timepoints (6-7-8 days). Data are reported as mean ± SD derived from three independent experiments.

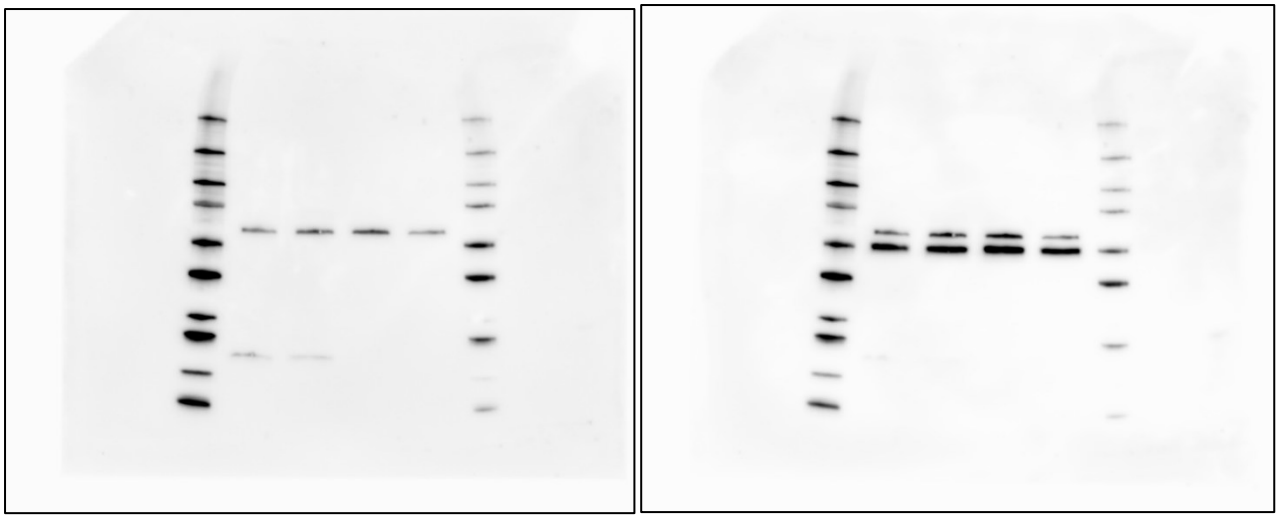

Fig. S2 Uncropped images of western blot analysis. A- p16 expression in G63, G65, G41 and G48 respectively. B- Actin β expression in G63, G65, G41 and G48 respectively. An aspecific band is evident above the housekeeping (50 kD). After several tests we demonstrated that it is caused by the marker and do not interfere with the expression of the other proteins.

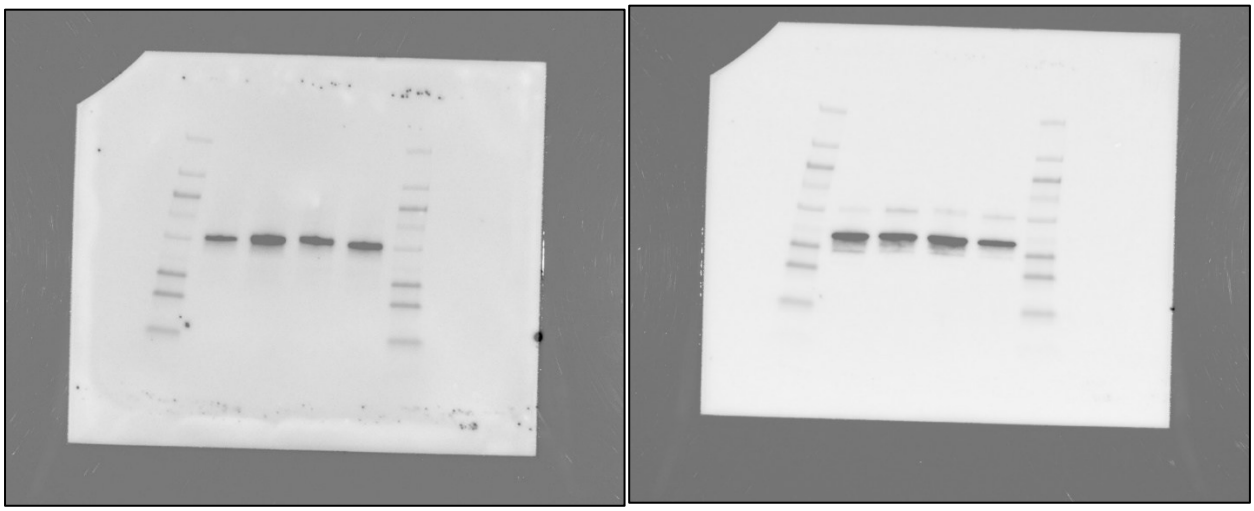

Fig. S3 Uncropped images of western blot analysis. A- p53 expression in G63, G48, G41 and G65 respectively. B- GAPDH (housekeeping) expression in G63, G48, G41 and G65 respectively.